J. Fluid Mech. (1990), *vol.* 221, *pp.* 233–261
Printed in Great Britain

Mixed nonlinearity and double shocks in superfluid helium

By M. S. CRAMER AND R. SEN†
Department of Engineering Science and Mechanics, Virginia Polytechnic Institute and State University, Blacksburg, VA, USA

(Received 12 December 1989)

We examine weak second-sound waves in He II at temperatures and pressures near one of the zeros of the Khalatnikov steepening parameter Γ. An extension of the reductive perturbation scheme of Taniuti & Wei is employed to derive the cubic Burgers' equation governing these waves. It is shown that mixed nonlinearity may occur in disturbances in which the local value of Γ remains strictly positive or strictly negative. Further new results include expressions for the shock speed, shock structure and the conditions under which the shock thickness increases, rather than decreases, with strength. The fundamental existence conditions for temperature shocks are also delineated and related to the shock disintegration process observed in experimental studies.

1. Introduction

At a temperature of approximately 2.17 K ordinary liquid helium (He I) undergoes a transition to a second phase referred to as He II or superfluid helium. The unusual properties of superfluid helium have been documented extensively; recent surveys have been given by Roberts & Donnelly (1974), Liepmann & Laguna (1984), Liepmann & Torczynski (1985), Donnelly & Swanson (1986) and Fiszdon & Vogel (1986). One of the best-known properties is the existence of a second sound mode in addition to ordinary sound. In He II the ordinary sound mode (first sound) carries perturbations in the pressure and density but the entropy is approximately constant. In contrast, the second sound mode carries perturbations in the entropy and temperature while the pressure and density remain constant.

Nonlinear effects on the sound speeds were described by Khalatnikov (1952) who gave the first correction to the linear theory of both first and second sound. The expression obtained for second sound is equivalent to

$$u_T\left\{1+\frac{c_{v0}\Gamma_0}{s_0\alpha_0}\frac{T-T_0}{T_0}+O\left[\left(\frac{T-T_0}{T_0}\right)^2\right]\right\}, \tag{1.1}$$

where c_v is the specific heat at constant volume, s is the entropy, T is the absolute temperature, $0 \leqslant \alpha \equiv \rho_s/\rho \leqslant 1$ is the mass fraction of superfluid, ρ_s is the superfluid density, ρ is the liquid density and

$$u_T \equiv s_0\left(\frac{\alpha_0}{1-\alpha_0}\frac{T_0}{c_{v0}}\right)^{\frac{1}{2}} \tag{1.2}$$

† Present address: Community Noise Research, Boeing Commercial Airplane Company, Seattle, WA 98124, USA.

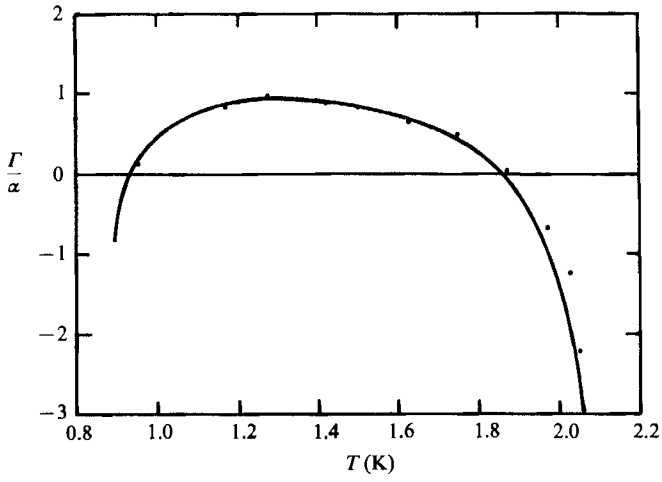

FIGURE 1. Variation of Khalatnikov steepening parameter Γ/α. Dots represent the data of Dessler & Fairbank (1956).

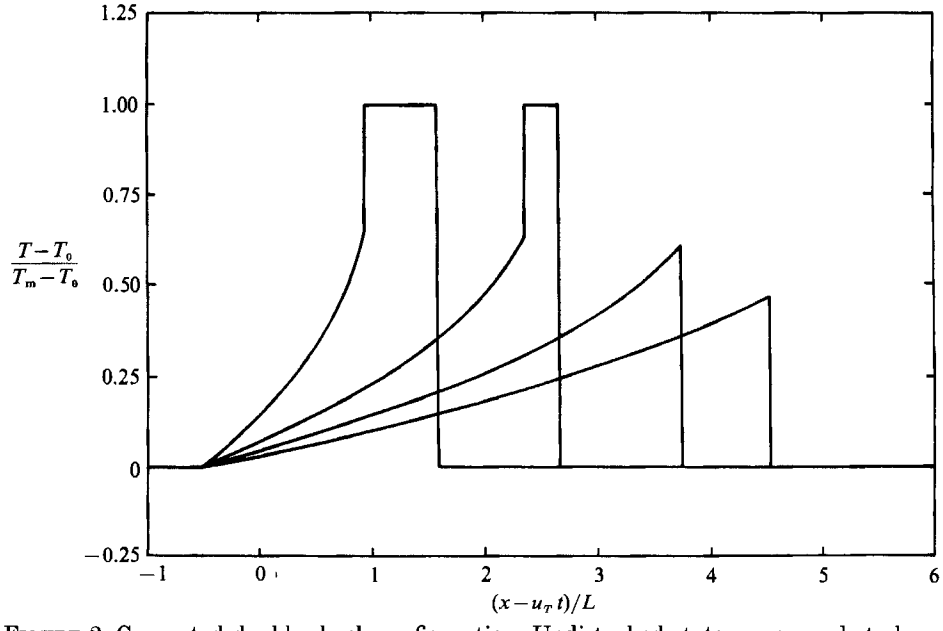

FIGURE 2. Computed double-shock configuration. Undisturbed state corresponds to low pressure and $T_0 = 1.85$ K, $w = 0$. The maximum temperature of the square pulse is $T_m = 1.883$ K. Values of $\Gamma_0 = 0.1046$ and $A = -0.9322$ were employed. The rear shock is sonic.

is the speed of second sound in the linear approximation. The quantity Γ is the usual first-order or quadratic nonlinearity coefficient given by

$$\Gamma \equiv \frac{\alpha s T}{c_v} \frac{\partial}{\partial T}\left\{\ln\left(u_T^3 \frac{c_v}{T}\right)\right\}, \tag{1.3}$$

where the differentiation in (1.3) is carried out at constant pressure. In the above equations and all that follow, the subscript 0 denotes quantities evaluated at the undisturbed state. The variation of Γ with temperature is shown in figure 1. For temperatures between approximately 0.95 and 1.88 K, Γ is positive. In this range second-sound wavefronts steepen forward to form shock waves which heat the

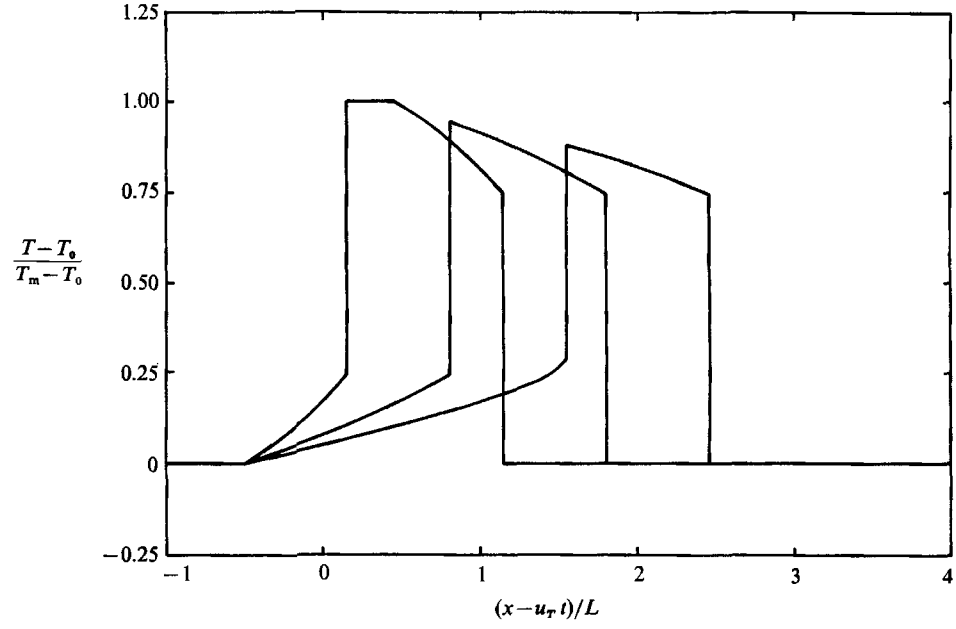

FIGURE 3. Computed double-shock configuration. Undisturbed state corresponds to low pressure, $T_0 = 1.85$ K, $w = 0$. The maximum temperature of the square pulse is $T_m = 1.9$ K. Values of $\Gamma_0 = 0.1046$ and $A = -0.9322$ were employed. Both shocks are sonic.

helium. Situations involving forward steepening will be referred to as those of positive nonlinearity. It is clear that this is analogous to the steepening found in the ordinary gasdynamics of dilute gases. The region where $\Gamma < 0$ corresponds to backward steepening and the formation of shocks which cool rather than heat the helium; we refer to this as negative nonlinearity. Backward steepening has no counterpart in perfect-gas theory. However, recent studies have revealed that negative nonlinearity may occur in a number of other areas of classical physics. A comprehensive survey has been given by Thompson, Carofano & Kim (1986).

Inspection of figure 1 suggests that the superfluid may be shocked from a region of positive to negative nonlinearity by appropriate choices of the undisturbed state and the shock strength. Recent experiments by Turner (1979, 1981, 1983) show that second-sound shocks suffer a partial disintegration when this occurs. For temperature raising shocks, the resultant waveform was seen to be a shock followed by a smooth heating wave. In Turner's experiments, the heat input was such that the wave would propagate as a square wave in the absence of nonlinear effects. These experiments, as well as those of Torczynski, Gerthsen & Roesgen (1984), reveal shocks at both the front and tail of the wave; these were temperature-raising and temperature-lowering shocks, respectively. Turner (1979) termed this a double-shock configuration and argued that this occurs when Γ changes sign from one part of the wave to the other. The partial disintegration and double-shock configuration are depicted in figures 2 and 3.

The purpose of the present study is to determine the equation governing mixed nonlinearity in weak second-sound waves. It is clear that (1.1) cannot provide such a description. The nonlinearity coefficient Γ_0 is determined once and for all by the undisturbed state: waves simply steepen forward or backward depending on the sign of Γ_0. Inspection of figure 1 shows that a disturbance of small amplitude will result in mixed nonlinearity only if the undisturbed state is sufficiently close to that where

Γ vanishes. Thus, the present study will require that Γ and the wave amplitudes are related by

$$\Gamma_0 = O\left(\frac{T-T_0}{T_0}\right) = o(1). \tag{1.4}$$

The equation governing the lowest-order disturbances will be derived by approximating the exact conservation equations of superfluid helium. Although the reductive perturbation technique of Taniuti & Wei (1968) yields the wavespeed (1.1) when $\Gamma_0 = O(1)$ and the $\Gamma_0 = 0$ extension by Teymur & Suhubi (1978) can be applied to a restricted class of problems, no general techniques are available when (1.4) holds. In response to this, the present authors have developed a general extension of the technique of Taniuti & Wei and apply it to He II. The general algorithm is stated in the Appendix.

The general formulation and assumptions are stated in §2. The equation governing non-dissipative second-sound disturbances and the corresponding nonlinear sound speed are given in §3. In §4 dissipative effects are treated. The dissipative results are then used to derive the shock speed and the fundamental existence conditions for shock waves. Non-classical features of the dissipative structure are also given. In §5, a brief discussion of the shock dynamics and the evolution of heat pulses is presented. Finally, in §6 we compare our results to the available experimental data.

The evolution equation derived here is seen to be an extension of Burgers' equation which includes both cubic and quadratic nonlinearity. The solutions to this equation have been described in detail in previous investigations and, in many cases, the reader will be referred to these studies. However, the solutions were presented in the context of Navier–Stokes fluids and a number of notation and convention changes are required to obtain results for the superfluid. To minimize the additional effort required and to keep the present study reasonably self-contained, some results will be recast and discussed in the context of He II.

2. Formulation

The macroscopic description of superfluid helium is through the Landau two-fluid equations, see e.g. Landau & Lifshitz (1959), Khalatnikov (1965) or Putterman (1974). Many treatments take the dependent variables in these equations to be the pressure p, temperature T, the velocity of the normal fluid $\boldsymbol{v}_n$ and the velocity of the superfluid component $\boldsymbol{v}_s$. For the present purposes we find it more convenient to use the density ρ, the entropy s, the barocentric or bulk velocity

$$\boldsymbol{v} \equiv \frac{\rho_n}{\rho}\boldsymbol{v}_n + \frac{\rho_s}{\rho}\boldsymbol{v}_s$$

and the slip or counterflow velocity between the normal and superfluid components $\boldsymbol{w} \equiv \boldsymbol{v}_n - \boldsymbol{v}_s$. Here $\rho_n = \rho - \rho_s$ denotes the density of the normal component. We further assume the flow to be non-dissipative and one-dimensional. The exact two-fluid equations may then be written

$$\rho_t + v\rho_x + \rho v_x = 0, \tag{2.1}$$

$$v_t + vv_x + \{w^2[\rho\alpha_\rho(1-2\alpha) + \alpha(1-\alpha)] + p_\rho\}\frac{\rho_x}{\rho} + \left(\frac{p_s}{\rho} + (1-2\alpha)\,\alpha_s w^2\right)s_x + 2\left\{\alpha(1-\alpha) + \frac{1}{\rho}p_w + (1-2\alpha)\,\alpha_w w^2\right\}ww_x = 0, \tag{2.2}$$

$$s_t + ws(\alpha + \rho\alpha_\rho)\frac{\rho_x}{\rho} + \{v + w(s\alpha)_s\}s_x + s\{\alpha + 2\alpha_w w^2\}w_x = 0, \tag{2.3}$$

$$\left(1 - \frac{2\alpha_w w^2}{1-\alpha}\right)w_t + \left\{\frac{\rho s T_\rho}{1-\alpha} + w^2\left(\alpha + \frac{s\alpha\alpha_s}{1-\alpha} + \rho\alpha_\rho\frac{2 + s\alpha_s - 3\alpha}{1-\alpha}\right)\right\}\frac{\rho_x}{\rho}$$
$$+ wv_x\left(1 + \frac{\rho\alpha_\rho}{1-\alpha}\right) + \frac{sT_s + w^2\alpha_s(s\alpha_s - 2\alpha + 2)}{1-\alpha}s_x$$
$$+ \left\{v\left(1 - \frac{2\alpha_w w^2}{1-\alpha}\right) + w\left(3\alpha + \frac{s}{1-\alpha}(2T_w + \alpha\alpha_s) + 2w^2\alpha_w\frac{s\alpha_s - 3\alpha + 2}{1-\alpha}\right)\right\}w_x = 0, \tag{2.4}$$

where the subscripts t, x, ρ, s and w denote differentiation with respect to time, position, density, entropy and the square of the slip velocity, i.e. w^2. Equations (2.1) and (2.2) are recognized as the usual mass and momentum balance for the bulk fluid. The third equation, (2.3), is the entropy balance and (2.4) will be referred to as the slip equation. The latter was derived from the momentum equation for the superfluid component. Equations (2.1)–(2.4) comprise four equations for the scalar fields $\rho(x,t)$, $v(x,t)$, $s(x,t)$ and $w(x,t)$ once the constitutive relations

$$\alpha = \alpha(\rho, s, w^2), \quad p = p(\rho, s, w^2), \quad T = T(\rho, s, w^2)$$

are specified. We follow previous investigators in assuming α, p, T to be analytic functions of w^2.

To complete our description, we note that the chemical potential μ of the superfluid may be defined such that

$$\mathrm{d}\mu = \frac{\mathrm{d}p}{\rho} - s\,\mathrm{d}T + \tfrac{1}{2}(\alpha - 1)\,\mathrm{d}w^2$$

from which the following Maxwell relations may be derived:

$$\left.\frac{\partial s}{\partial p}\right|_{T,w^2} = -\frac{\beta}{\rho}, \quad \left.\frac{\partial s}{\partial w^2}\right|_{p,T} = -\frac{1}{2}\left.\frac{\partial\alpha}{\partial T}\right|_{p,w^2}, \quad \left.\frac{\partial\rho}{\partial w^2}\right|_{T,p} = -\tfrac{1}{2}\rho^2\left.\frac{\partial\alpha}{\partial p}\right|_{T,w^2}, \tag{2.5}$$

where

$$\beta \equiv -\frac{1}{\rho}\left.\frac{\partial\rho}{\partial T}\right|_{p,w^2} \tag{2.6}$$

will be referred to as the coefficient of thermal expansion. The relation between p, T, w^2 and ρ, s, w^2 is given by the differential relations

$$\mathrm{d}p = \frac{\beta T\rho a^2}{c_p}\mathrm{d}s + a^2\,\mathrm{d}\rho + \frac{\beta T\rho a^2}{2c_p}\left(\left.\frac{\partial\alpha}{\partial T}\right|_{p,w^2} + \frac{c_p\rho}{\beta T}\left.\frac{\partial\alpha}{\partial p}\right|_{T,w^2}\right)\mathrm{d}w^2, \tag{2.7}$$

$$\mathrm{d}T = \frac{T}{c_v}\mathrm{d}s + \frac{\beta T a^2}{\rho c_p}\mathrm{d}\rho + \frac{T}{2c_v}\left(\left.\frac{\partial\alpha}{\partial T}\right|_{p,w^2} + \frac{\beta a^2\rho}{\gamma}\left.\frac{\partial\alpha}{\partial p}\right|_{T,w^2}\right)\mathrm{d}w^2, \tag{2.8}$$

where c_p is the specific heat at constant pressure, γ is the ratio of specific heats $= c_p/c_v$ and

$$a \equiv \left(\left.\frac{\partial p}{\partial\rho}\right|_{s,w^2}\right)^{\frac{1}{2}} \tag{2.9}$$

will be referred to as the speed of first sound. It may also be shown that the familiar identity

$$a^2 = c_p\frac{\gamma - 1}{\beta^2 T} \tag{2.10}$$

holds in the present case. Equations (2.7) and (2.8) are recognized as extensions of the $T\,ds$ equations of simple fluids and follow directly from the constitutive assumptions on p, T, α and the Maxwell relations.

It is generally recognized that the coefficient of thermal expansion (2.6) is relatively small for temperatures of interest in the present study and this assumption is inherent in most derivations of the nonlinear speed of second sound; see e.g. the discussion provided by Putterman (1974). In particular (1.1) and (1.2) were obtained subject to this condition along with the small-disturbance approximation. In order to simplify our presentation we shall follow previous investigators and ignore terms involving β in the bulk of our computations. Once the final result is established, the corrections for small but finite β will be described. In order to satisfy (2.10), the first-sound speed (2.9) will be regarded as finite as $\beta \to 0$, which implies that γ may be taken to be unity for the present purposes.

Most of the assumptions to be applied here are essentially the same as those of the first-order theory. That is, β will be regarded as negligibly small, the undisturbed state is taken to be at rest ($v = w = 0$) and uniform ($s_0, \rho_0 =$ constants), and the second-sound disturbances will be taken to be small. The additional feature of the present study is that the undisturbed state will be taken to be near either of the zeros of Γ; the precise ordering is given in (1.4).

3. Derivation of the evolution equation

We begin by introducing non-dimensional variables

$$\bar{x} = \frac{x}{L}, \quad \bar{t} = \frac{tu_T}{L}, \quad \bar{\rho} = \frac{\rho}{\rho_0}, \quad \bar{v} = \frac{v}{u_T}, \quad \bar{s} = \frac{s}{s_0}, \quad \bar{w} = \frac{w}{u_T}, \quad \bar{T} = \frac{T}{T_0}, \quad \bar{a} = \frac{a}{u_T}, \tag{3.1}$$

where L is a lengthscale associated with an initial or boundary condition. Overbars will be used to denote non-dimensional quantities throughout. When the assumption that β is negligible is applied, the non-dimensional form of the conservation equations (2.1)–(2.4) is found to be

$$u_{i\bar{t}} + A_{ij}(u_p)\, u_{j\bar{x}} = O(|u_k - u_k^0|^4), \tag{3.2}$$

where all indices range from 1 to 4, the Einstein summation convention is applied, $u_i = (\bar{\rho}, \bar{v}, \bar{s}, \bar{w})$ and

$$A_{11} = \bar{v}, \quad A_{12} = \bar{\rho}, \quad A_{13} = A_{14} = 0,$$

$$A_{21} = \frac{\bar{a}^2}{\bar{\rho}} + \frac{\alpha(1-\alpha)\,\bar{w}^2}{\bar{\rho}} + \bar{w}^2(1-2\alpha)\,\alpha_{\bar{\rho}},$$

$$A_{22} = \bar{v}, \quad A_{23} = \bar{w}^2(1-2\alpha)\,\alpha_{\bar{s}}, \quad A_{24} = \frac{2\bar{w}}{\bar{\rho}}\bar{p}_{\bar{w}} + 2\alpha\bar{w}(1-\alpha),$$

$$A_{31} = \frac{\alpha\bar{w}\bar{s}}{\bar{\rho}} + \bar{w}\bar{s}\alpha_{\bar{\rho}}, \quad A_{32} = 0, \quad A_{33} = \bar{v} + \alpha\bar{w} + \bar{w}\bar{s}\alpha_{\bar{s}}, \quad A_{34} = \alpha\bar{s} + 2\bar{w}^2\bar{s}\alpha_{\bar{w}}, \tag{3.3}$$

$$A_{41} = \frac{\bar{w}^2\bar{s}}{\bar{\rho}}\alpha_{\bar{s}} \frac{\alpha}{1-\alpha} + \frac{\bar{w}^2\bar{s}}{1-\alpha}\alpha_{\bar{s}}\alpha_{\bar{\rho}} + \bar{w}^2\left(\frac{3\alpha-2}{\alpha-1}\right)\alpha_{\bar{\rho}} + \frac{\alpha\bar{w}^2}{\bar{\rho}}, \quad A_{42} = \bar{w} + \frac{\bar{\rho}\bar{w}}{1-\alpha}\alpha_{\bar{\rho}},$$

$$A_{43} = 2\bar{w}^2\alpha_{\bar{s}} + \frac{\bar{w}^2\bar{s}}{1-\alpha}(\alpha_{\bar{s}})^2 + \frac{s_0 T_0}{u_T^2}\frac{\bar{s}}{1-\alpha}\left(1 + \frac{2\bar{w}^2}{1-\alpha}\alpha_{\bar{w}}\right)\bar{T}_{\bar{s}},$$

$$A_{44} = \bar{v} + 3\alpha\bar{w} + \frac{\alpha\bar{w}\bar{s}}{1-\alpha}\alpha_{\bar{s}} + \frac{2s_0 T_0}{u_T^2}\frac{\bar{s}\bar{w}}{1-\alpha}\bar{T}_{\bar{w}}.$$

The quantity u_i^0 refers to the values of u_i evaluated at the undisturbed state, i.e. $u_i^0 = (1, 0, 1, 0)$.

When the perturbation technique described in the Appendix is applied to the system (3.2), (3.3) we find that

$$\frac{w}{u_T} \approx \frac{s-s_0}{\alpha_0 s_0} \approx \frac{c_{v0}}{\alpha_0 s_0}\frac{T-T_0}{T_0} \approx \epsilon U(X,\tau), \tag{3.4}$$

where the shape function U satisfies the cubic Burgers' equation

$$U_\tau + (\hat{\Gamma} + \tfrac{1}{2}\Lambda U)\, UU_X = 0. \tag{3.5}$$

Here ϵ is a non-dimensional measure of the small initial amplitude, $\tau = \epsilon^2 \bar{t}$ is the slow time and the wave coordinate X is simply $\bar{x} - \bar{t}$ due to the scaling on $\bar{t}$. The nonlinearity coefficients were found to be

$$\hat{\Gamma} = \frac{1}{\epsilon}\left(3\alpha_0 + \frac{3}{2}\frac{s_0\alpha_s}{1-\alpha_0} + \frac{1}{2}\frac{\alpha_0 s_0 c_{v0}}{T_0}T_{ss}\right), \tag{3.6}$$

$$\begin{aligned}\Lambda = {} & -18\alpha_0^2 - \frac{6\alpha_0(1-\alpha_0)u_T^2}{a_0^2-u_T^2} - \frac{12\alpha_0 s_0}{1-\alpha_0}\alpha_s - \frac{6s_0^2}{1-\alpha_0}(\alpha_s)^2 + \frac{3\alpha_0 s_0^2}{1-\alpha_0}\alpha_{ss} \\ & + \frac{3u_T^2}{\alpha_0(1-\alpha_0)}\alpha_w + \frac{\alpha_0^2 s_0^2 c_{v0}}{2T_0}T_{sss} - \frac{6\rho_0 u_T^2}{a_0^2-u_T^2}\alpha_\rho - \frac{3\rho_0^2 u_T^2}{2\alpha_0(1-\alpha_0)(a_0^2-u_T^2)}(\alpha_\rho)^2,\end{aligned} \tag{3.7}$$

where all partial derivatives appearing in (3.6) and (3.7), e.g. α_s, T_{ss}, etc., are to be evaluated at the undisturbed state. Results (2.7), (2.8) and (1.2) may be used to verify that $\hat{\Gamma}$ is just Γ_0/ϵ, where Γ is given in (1.3). The second nonlinearity coefficient (3.7) may also be converted to a quantity involving only derivatives with respect to p, T and w^2; the resultant expression for Λ is

$$\begin{aligned}\Lambda = {} & -18\alpha_0^2 - 6\alpha_0(1-\alpha_0)\frac{u_T^2}{a_0^2-u_T^2} + \frac{3\alpha_0 T_0 s_0}{(1-\alpha_0)c_{v0}}\left\{\frac{s_0}{c_{v0}}\left(1 - \frac{T_0}{c_{v0}}\frac{\partial c_v}{\partial T}\right) - 4\right\}\frac{\partial \alpha}{\partial T} \\ & + \frac{3}{2}\left(\frac{s_0}{c_{v0}}\right)^2 \frac{T_0^2(4\alpha_0-3)}{(1-\alpha_0)^2}\left(\frac{\partial \alpha}{\partial T}\right)^2 + \frac{3\alpha_0 T_0^2}{1-\alpha_0}\left(\frac{s_0}{c_{v0}}\right)^2 \frac{\partial^2 \alpha}{\partial T^2} \\ & - \frac{6\rho_0 u_T^2 a_0^2}{a_0^2-u_T^2}\frac{\partial \alpha}{\partial p} - \frac{3u_T^4\rho_0^2}{2\alpha_0(1-\alpha_0)}\frac{a_0^2}{a_0^2-u_T^2}\left(\frac{\partial \alpha}{\partial p}\right)^2 \\ & + \frac{1}{2}\left(\frac{\alpha_0 s_0}{c_{v0}}\right)^2 \left\{1 - \frac{4T_0}{c_{v0}}\frac{\partial c_v}{\partial T} + 3\left(\frac{T_0}{c_{v0}}\frac{\partial c_v}{\partial T}\right)^2 - \frac{T_0^2}{c_{v0}}\frac{\partial^2 c_v}{\partial T^2}\right\} + \frac{3u_T^2}{\alpha_0(1-\alpha_0)}\frac{\partial \alpha}{\partial w^2},\end{aligned} \tag{3.8}$$

where α and c_v are now regarded as functions of p, T and w^2. To the accuracy inherent in (3.5) we may replace $\partial c_v/\partial T$ in (3.8) by

$$\frac{c_{v0}}{T_0}\left(1 + 6\frac{c_{v0}}{s_0} + \frac{3T_0}{\alpha_0(1-\alpha_0)}\frac{\partial \alpha}{\partial T}\right).$$

This is equivalent to the condition of small Γ_0 (1.4).

Numerical values for Λ in the neighbourhood of the high-temperature zero of Γ have been computed and are displayed in table 1. Most of the quantities appearing

T (K)	Γ	A	$\left.\frac{\alpha s T}{c_v}\frac{\partial \Gamma}{\partial T}\right\|_p$
1.850	1.0×10^{-1}	−1.07	−0.68
1.884	-7.4×10^{-3}	−0.93	−0.70
1.900	-6.0×10^{-2}	−0.87	−0.71

TABLE 1. Estimates for Γ, A and the variation of Γ with temperature near 1.88 K and $p \approx 0$ bar. The values at 1.884 K were obtained by linear interpolation of the values at 1.85 K and 1.90 K. A more accurate graphical interpolation yields $\Gamma \approx 0$ at 1.884 K.

in (3.8) were obtained directly from the tabular data of Maynard (1976). We note that Maynard does not provide estimates for the first and second derivatives of α and c_v. In each case these derivatives were computed from a central-differencing operator applied to the data in table I of Maynard. In this low-pressure case, the derivative $\partial\alpha/\partial p$ was taken from the saturation data in his table III. Maynard's data also give no information concerning the $\partial\alpha/\partial w^2$ term in (3.8). The dependence of α on w is difficult to measure by current methods and no generally accepted data are available. However, an analytical expression for the dependence of ρ_n on w has been provided by Khalatnikov (1965). Here we employ this result and further assume that the roton contribution to ρ_n is the dominant one. The resultant small-w approximation to α may then be written

$$\alpha \approx 1-(1-\alpha_0)\frac{\rho_0}{\rho}\left(1+B\frac{w^2}{T^2}\right), \tag{3.9}$$

where, for helium, $B \approx 2.13\times10^{-3}$ (s K/m)^2. An equivalent expression was employed by Atkin & Fox (1984). It should be noted that (3.9) is also consistent with the experimental results of Kojima *et al.* (1976). Differentiation and use of (2.5) yields

$$\left.\frac{3u_T^2}{\alpha_0(1-\alpha_0)}\frac{\partial\alpha}{\partial w^2}\right|_{p,\,T} \approx -\frac{3}{2}\frac{\rho_0 u_T^2 \alpha_p}{a_0}-3\frac{u_T^2 B}{\alpha_0 T_0^2}$$

as the expression for the last term in (3.8). We note that many authors have neglected the dependence of α on w. When we compare the typical numerical values of the last term in (3.8) (approximately equal to -1) to the final value of A in table 1, we conclude that the contrary is true; namely, the dependence of α on w plays a critical role in the dynamics when $\Gamma \approx 0$. In §6, we shall show that the combination of (3.8) and (3.9) yields results that are in complete agreement with the available experimental data, thus validating the use of Khalatnikov's formula (3.9).

Because the errors inherent in most of the terms in (3.8) are relatively small, the results presented here and in the following sections can serve as the basis for the experimental verification or determination of the $\rho_n = \rho_n(w)$ relation, at least in the neighbourhood of the $\Gamma = 0$ locus. This method will be described in §6.

The local speed of second sound is found by applying the method of characteristics to (3.5). In terms of a stationary reference frame and the physical variables we find

$$\begin{aligned}\sigma &= u_T\left\{1+\Gamma_0\frac{w}{u_T}+\tfrac{1}{2}A\left(\frac{w}{u_T}\right)^2+O\left[\left(\frac{w}{u_T}\right)^3\right]\right\}\\ &= u_T\left\{1+\frac{\Gamma_0 c_{v0}}{\alpha_0 s_0}\frac{T-T_0}{T_0}+\tfrac{1}{2}A\left(\frac{c_{v0}}{\alpha_0 s_0}\right)^2\left(\frac{T-T_0}{T_0}\right)^2+O\left[\left(\frac{T-T_0}{T_0}\right)^3\right]\right\}.\end{aligned} \tag{3.10}$$

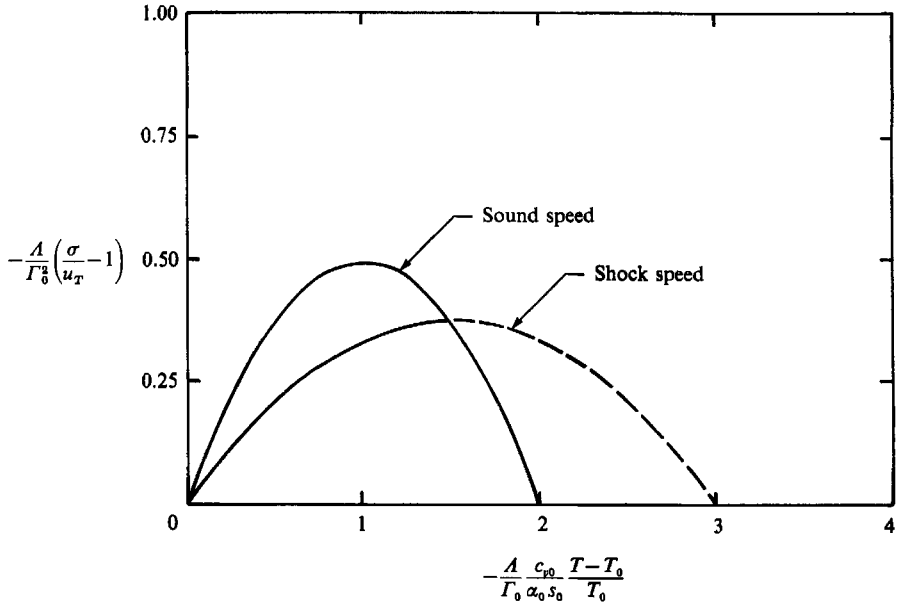

FIGURE 4. Variation of shock and second-sound speeds with disturbance amplitude. The curve for the shock speed corresponds to $w_1 = 0, T_1 = T_0$ and the horizontal coordinate should be interpreted as the disturbance immediately after the shock.

A non-dimensional version of (3.10) is plotted in figure 4. An analogous wavespeed relation was derived by Cramer & Kluwick (1984) in the context of single-phase gases with large specific heats and by Garrett (1981) in the context of fourth sound in ^{3}He-B. The existence of a maximum wavespeed was also recognized by Turner (1979). The effective steepening or nonlinearity coefficient corresponding to (3.5) is

$$\sigma' = \frac{\mathrm{d}\sigma}{\mathrm{d}w} = \Gamma_0 + \Lambda\frac{w}{u_T}$$

$$= \Gamma_0 + \frac{\Lambda c_{v0}}{\alpha_0 s_0}\frac{T-T_0}{T_0}. \tag{3.11}$$

Forward steepening corresponds to $\sigma' > 0$ and backward steepening corresponds to $\sigma' < 0$. An important feature not anticipated in previous investigations is revealed by comparing (3.11) to the expression for the local value of Γ as defined by (1.3). To the present accuracy, the latter reads

$$\Gamma = \Gamma_0 + T_0\frac{\partial\Gamma}{\partial T}\frac{T-T_0}{T_0} + O\left[\left(\frac{T-T_0}{T_0}\right)^2\right], \tag{3.12}$$

where

$$T\frac{\partial\Gamma}{\partial T} = T\frac{\partial\alpha}{\partial T}\left\{3+\frac{3}{2}\frac{1}{1-\alpha}+\frac{1}{2}\frac{4-\alpha}{1-\alpha}\frac{s}{c_v}\left(1-\frac{T}{c_v}\frac{\partial c_v}{\partial T}\right)\right\}$$

$$+\frac{3}{2}\frac{s}{c_v}\frac{T^2}{1-\alpha}\frac{\partial^2\alpha}{\partial T^2}+\frac{3}{2}\frac{s}{c_v}\frac{T^2}{(1-\alpha)^2}\left(\frac{\partial\alpha}{\partial T}\right)^2+\tfrac{1}{2}\alpha\left(1-2\frac{sT}{c_v^2}\frac{\partial c_v}{\partial T}\right)\left(1-\frac{T}{c_v}\frac{\partial c_v}{\partial T}\right)-\frac{\alpha s T^2}{2c_v^2}\frac{\partial^2 c_v}{\partial T^2}. \tag{3.13}$$

A comparison of (3.13) to (3.8) shows that

$$\Lambda + \frac{\alpha_0 s_0 T_0}{c_{v0}} \frac{\partial \Gamma}{\partial T};$$

this fact is also evident from table 1. We therefore conclude that the point at which the steepening coefficient σ' changes sign is not the same as that at which the local value of Γ changes sign. Thus, cooling shocks may be formed in waves having $\Gamma > 0$ at every point. One example is the temperature-lowering shock seen in figure 2. To further illustrate this we have computed the temperature at which σ' and Γ, as defined in (3.11) and (3.12), change sign for an undisturbed state $T_0 = 1.85$ K and $p \approx 0$. We find that σ' changes sign at approximately 1.872 K and the local value of Γ changes sign at 1.884 K.

The differences between the nonlinearity parameter based on (3.13) and Λ are due to higher-order powers of the slip velocity in (3.3) and the generation of disturbances in the pressure and bulk velocity at first, rather than lowest, order by nonlinear effects. The latter effect is reflected in the fact that the terms involving the first-sound speed a_0 and the derivatives of α with respect to p cannot be generated by the derivatives of (1.3) with respect to temperature. The reason for the differences is that (1.3) is only an approximation to the exact steepening coefficient. In the present case, higher-order terms which are properly neglected in the Khalatnikov theory are seen to make a contribution which is non-negligible in the present $\Gamma_0 = O(\epsilon)$ theory.

The nonlinear steepening associated with (3.5) and (3.10) is known to differ qualitatively from that observed when $\Gamma = O(1)$. The details of this steepening and shock formation have been given by Garrett (1981) for oscillatory signals and by Cramer & Kluwick (1984) for the case of pulses of finite width.

As discussed in §1, the results presented here neglect the effects of the coefficient of thermal expansion β. However, any extension to include β will leave the general form of (3.5) unchanged provided that the shift in the linear wavespeed is taken into account. Modifications to the coefficients in (3.5) are first needed when the appropriate non-dimensional version of β is of order ϵ. Even in this case, the result of primary interest, the second nonlinearity coefficient Λ, remains unchanged. The main modification needed is in $\hat{\Gamma}$, which should be replaced by the version containing the first correction for non-zero β. In addition, the linear speed should contain the well-known $O(\beta^2) = O(\epsilon^2)$ correction.

4. Dissipation and shock structure

The dissipative fluxes for He II are normally taken to be linear in gradients of the field variables; see e.g. Khalatnikov (1965) or Putterman (1974). If we further assume that the dissipation is weak, we find that the extension of (3.2) may be written

$$u_{i\bar{t}} + A_{ij}(u_p)\, u_{j\bar{x}} = D_{ij}\, u_{j\bar{x}\bar{x}} + \ldots, \tag{4.1}$$

where the left-hand side is identical to (3.2) and the dots denote terms of fourth order in the amplitude and higher order in the dissipation. Only the lowest-order effects of the weak dissipation will be considered here. As a result, the dissipation matrix D_{ij} is a constant.

When the dissipation is strong compared with the nonlinear steepening the disturbance will damp out before the latter becomes noticeable at lowest order. If the dissipation is relatively weak, the nonlinear steepening generates shock waves. The

lengthscale associated with the shock thickness is normally such that the nonlinear and dissipative effects are in balance. As in the usual derivation of Burgers' equation, we shall confine our attention to cases where the dissipation and nonlinear steepening occur at roughly the same rates. The precise condition is that

$$l_i D_{ij} r_j = O(\epsilon^2), \tag{4.2}$$

where l_i and r_i are the left and right eigenvectors of $A_{ij}(u_p^0)$ defined by (A 6). Under these conditions, it may be shown that the extension of (3.5) is

$$U_\tau + (\hat{\Gamma} + \tfrac{1}{2}\Lambda U) UU_X = \frac{\hat{\delta}}{2} U_{XX}, \tag{4.3}$$

where $\hat{\delta} \equiv \delta\epsilon^{-2}$ and

$$\begin{aligned} \delta &\equiv \frac{l_i D_{ij} r_j}{l_m r_m} \\ &= \frac{1}{Re} \frac{\alpha_0}{1-\alpha_0} \left\{ \frac{4}{3} + \frac{\eta_b}{\eta_0} + \frac{\rho_0}{\eta_0} (\rho_0 \zeta_3 - 2\zeta_1) + \frac{1-\alpha_0}{\alpha_0} \frac{1}{Pr} \right\}. \end{aligned} \tag{4.4}$$

The quantities η_0, η_b are the shear and bulk viscosities, respectively, and ζ_1, ζ_3 are the additional dissipation coefficients of the two-fluid model. The non-dimensional quantities Re and Pr are defined

$$Re \equiv \frac{u_T \rho_0 L}{\eta_0}, \quad Pr = \frac{\eta_0 c_{v0}}{k_0} \tag{4.5}$$

and are recognized as Reynolds and Prandtl numbers. In (4.5) the thermal conductivity is denoted by k_0 and the use of c_v instead of c_p reflects the small-β assumption. Because the dissipation is weak, the relation of U to the physical variables (3.4) holds without modification.

The diffusivity (4.4) agrees, as it should, with the usual attenuation coefficients for sound absorption. This is also consistent with the coefficient derived directly from the steady-flow shock structure equations by Turner (1979).

This form of the cubic Burgers' equation (4.3) was also derived by Cramer & Kluwick (1984) for the case of single-phase fluids which have a large heat capacity. Detailed numerical solutions were obtained by Cramer *et al.* (1986) for the unsteady evolution of square pulses involving double shocks. Lee-Bapty (1981) has provided an extensive analysis of the $\hat{\Gamma} \equiv 0$ version of (4.3), see also Crighton (1986) and Lee-Bapty & Crighton (1987). The work of Cramer & Kluwick (1984), Crighton (1986) and Cramer (1987) has demonstrated that the dissipative structure of shock waves associated with (4.3) can differ significantly from the well-known Taylor structure. In media admitting mixed nonlinearity, the dissipative structure plays an essential role in the determination of acceptable shock waves. For this reason, as well as the anticipated non-classical behaviour, the remainder of this section will summarize the main results for the structure as they apply to second sound.

Equation (4.3) describes the evolution of second-sound disturbances which propagate in the positive x-direction, i.e. to the right. The simplest model of the dissipative structure of such a right-moving shock is obtained by regarding the flow as steady in a reference frame moving at the shock speed

$$u_T(1 + \epsilon^2 S),$$

where S will be determined below. With this assumption we find that $U = U(\chi)$ satisfies the ordinary differential equation

$$U'' = \frac{2}{\delta}(-S + \hat{\Gamma}U + \tfrac{1}{2}\Lambda U^2)\,U', \tag{4.6}$$

where the primes denote differentiation with respect to $\chi \equiv X - \epsilon^2 S\bar{t}$. At this stage we make the well-known assumption that

$$\left.\begin{aligned} U &\to U_1 \quad \text{as} \quad \chi \to \infty, \\ U &\to U_2 \quad \text{as} \quad \chi \to -\infty, \end{aligned}\right\} \tag{4.7}$$

where U_1 and U_2 are the values of U upstream and downstream of the shock, respectively. Integration of (4.6) and application of (4.7) yields the shock speed

$$S = \tfrac{1}{2}\hat{\Gamma}(U_1 + U_2) + \tfrac{1}{6}\Lambda\{(U_1)^2 + U_1 U_2 + (U_2)^2\}. \tag{4.8}$$

The non-dimensional speed (4.8) may be converted to physical variables through use of the coordinate transformations and (3.4). When this is done we find that the dimensional shock speed σ_s is given by

$$\begin{aligned} \sigma_s &= u_T\left\{1 + \tfrac{1}{2}\Gamma_0\frac{w_1 + w_2}{u_T} + \tfrac{1}{6}\Lambda\frac{w_1^2 + w_1 w_2 + w_2^2}{u_T^2}\right\} \\ &= u_T\left\{1 + \frac{1}{2}\frac{\Gamma_0 c_{v0}}{\alpha_0 s_0}\left(\frac{T_1 - T_0}{T_0} + \frac{T_2 - T_0}{T_0}\right) + \tfrac{1}{6}\Lambda\left(\frac{c_{v0}}{\alpha_0 s_0}\right)^2\left[\left(\frac{T_1 - T_0}{T_0}\right)^2\right.\right. \\ &\quad \left.\left. + \left(\frac{T_1 - T_0}{T_0}\frac{T_2 - T_0}{T_0}\right) + \left(\frac{T_2 - T_0}{T_0}\right)^2\right]\right\}. \end{aligned} \tag{4.9}$$

The first term in (4.8) is recognized as the result of Khalatnikov (1952) and the second term is the required correction to the shock speed when $\Gamma_0 = O(\epsilon)$. A non-dimensional version of σ_s is plotted in figure 4 for the case of a shock propagating into a medium that is initially undisturbed, i.e. $w_1 = T_1 - T_0 = 0$.

Further integration of (4.6) yields the following implicit expressions for the shock structure:

$$\frac{w - w_1}{w_2 - w_1} = \frac{T - T_1}{T_2 - T_1} = \tfrac{1}{2}(G + 1), \tag{4.10}$$

$$\frac{x_s}{L_d} = \operatorname{sgn}(\Lambda)\left(\frac{\Gamma_0}{\Lambda}\frac{u_T}{w_2 - w_1}\right)^2 \xi, \tag{4.11}$$

where $\operatorname{sgn}(\Lambda)$ denotes the sign of Λ. The quantity L_d is a nonlinear diffusion length defined by

$$L_d \equiv \frac{6\eta_0|\Lambda|}{u_T \rho_0 \Gamma_0^2}\frac{\alpha_0}{1 - \alpha_0}\left\{\frac{4}{3} + \frac{\eta_b}{\eta_0} + \frac{\rho_0}{\eta_0}(\rho_0\zeta_3 - 2\zeta_1) + \frac{1 - \alpha_0}{\alpha_0}\frac{1}{Pr}\right\}, \tag{4.12}$$

and x_s is the dimensional distance as measured in the frame moving with the shock. The scaled position ξ and disturbance amplitude G are related by

$$\xi = \frac{1}{z^2 - 1}\left\{2\ln\frac{G + z}{z} + z\ln\frac{1 - G}{1 + G} - \ln(1 - G^2)\right\} \tag{4.13}$$

if $z\operatorname{sgn}(\Lambda) > 1$ and, when $z\operatorname{sgn}(\Lambda) = 1$,

$$\xi = \operatorname{sgn}(\Lambda)\left\{\tfrac{1}{2}\ln\frac{1 - G}{1 + G} - \operatorname{sgn}(\Lambda)\frac{G}{G + \operatorname{sgn}(\Lambda)}\right\}. \tag{4.14}$$

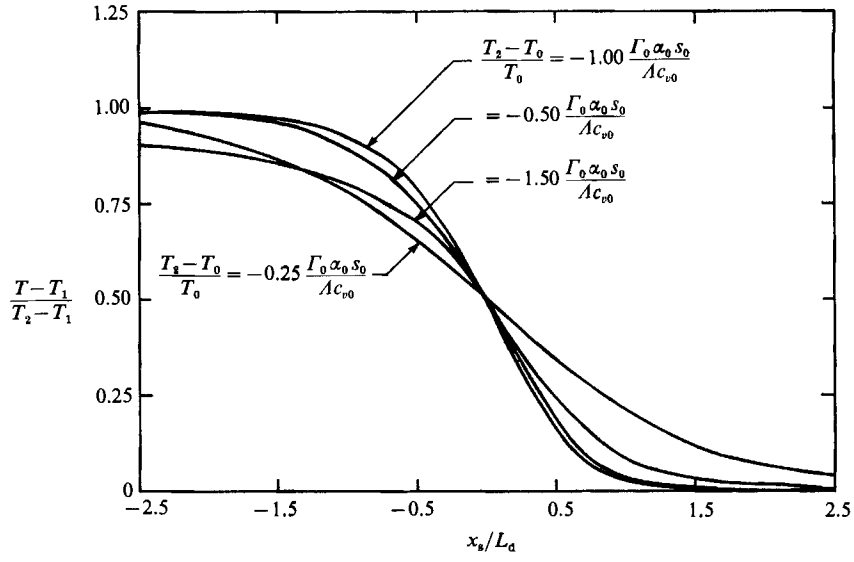

FIGURE 5. Dissipative shock structure for $\Gamma_0 > 0, \Lambda < 0, w_1 = 0, T_1 = T_0$. The sonic shock corresponds to the strength $-1.5\,\Gamma_0\alpha_0 s_0/\Lambda c_{v0}$.

The parameter z is related to the perturbations in w upstream and downstream of the shock by

$$z = 3+6\left(\frac{u_T}{w_2-w_1}\frac{\Gamma_0}{\Lambda}\right)\left(1+\frac{\Lambda}{\Gamma_0}\frac{w_1}{u_T}\right). \tag{4.15}$$

Plots of the structure in the case where the shock propagates into an undisturbed medium, i.e. $T_1 = T_0, w_1 = 0$, having $\Lambda < 0$ are given in figure 5.

Because no continuous solutions satisfying (4.6) and (4.7) exist for sgn $(\Lambda)\, z < 1$, we conclude that admissible second-sound shock waves must satisfy

$$z-1 = 2\frac{\dfrac{w_2-w_1}{u_T}\dfrac{\Lambda}{\Gamma_0}+3+3\dfrac{\Lambda}{\Gamma_0}\dfrac{w_1}{u_T}}{\dfrac{w_2-w_1}{u_T}\dfrac{\Lambda}{\Gamma_0}} \geqslant 0 \quad \text{for} \quad \Lambda > 0, \tag{4.16a}$$

$$z+1 = 2\frac{2\dfrac{w_2-w_1}{u_T}\dfrac{\Lambda}{\Gamma_0}+3+3\dfrac{\Lambda}{\Gamma_0}\dfrac{w_1}{u_T}}{\dfrac{w_2-w_1}{u_T}\dfrac{\Lambda}{\Gamma_0}} \leqslant 0 \quad \text{for} \quad \Lambda < 0. \tag{4.16b}$$

We note that the existence conditions (4.16) are independent of the dissipation parameters and may be applied in nondissipative calculations. It may also be shown that (4.16*a*, *b*) imply the speed-ordering relations

$$\left.\begin{aligned} \sigma_2 > \sigma_s \geqslant \sigma_1 \quad &\text{if} \quad \Lambda > 0 \\ \sigma_2 \geqslant \sigma_s > \sigma_1 \quad &\text{if} \quad \Lambda < 0, \end{aligned}\right\} \tag{4.17}$$

where σ_1, σ_2 are the nonlinear speeds (3.10) evaluated at the upstream and downstream conditions. Thus, second-sound waves behind the shock will always catch the shock and waves ahead of the shock will always be caught by it. The

equalities in (4.16) and (4.17) correspond to shock speeds identically equal to either the upstream or downstream wavespeed. We refer to such shocks as sonic and note that these are only possible when the nonlinearity is mixed, i.e. when σ' changes sign.

As an example of the application of the existence conditions (4.16) or (4.17), we consider the possibility of shocks having $w_1 = 0, \Gamma_0 = 0$, i.e. shocks having an upstream state exactly at the zero of the steepening parameter. Inspection of (4.16) shows that such a temperature shock is possible only if $\Lambda > 0$ (where both temperature-lowering and temperature-raising shocks are possible). A heuristic argument for the isolation of the high-temperature zero can be constructed by considering figure 1. Temperature-raising shocks always enter the region of $\Gamma < 0$, resulting in $\Gamma < 0$ everywhere inside the shock (provided the temperature distribution increases monotonically). Because the steepening is backward at every point, a temperature-raising shock is expected to break up into a centred fan. Similar remarks hold for temperature-lowering shocks. A somewhat more rigorous version of this argument can be constructed by considering (3.11). As a second example, we consider the types of shocks possible when $\Gamma_0 \neq 0$. We again take $w_1 = 0$ and consider only the high-temperature zero, i.e. $\Lambda < 0$. Inspection of (4.16*b*) shows that the only shocks possible when $\Gamma_0 > 0$ are temperature-raising shocks ($w_2 > 0$), and are temperature-lowering shocks ($w_2 < 0$) when $\Gamma_0 < 0$. This, of course, is in complete agreement with our intuition. However, each type will be limited in strength by the sonic shock condition given by the equality in (4.16*b*).

The structure of sonic shocks is given by (4.14). At the sonic side of the shock the approach to the asymptotes is algebraic rather than exponential. This relatively slow approach is clearly seen in figure 5. The non-classical nature of sonic shocks is further illustrated by an inspection of the shock thickness for undisturbed states in the neighbourhood of 1.88 K. In this region $\Lambda < 0$ and the sonic shock is the shock of maximum strength. Thus, the usual tendency of weak shocks to become thinner as the strength increases will be counterbalanced by the thickening associated with the algebraic approach inherent in (4.14). To put this on a quantitative basis we have computed the shock thickness based on the maximum-slope criterion. The dimensional thickness Δ is found to be

$$\frac{\Delta}{L_{\mathrm{d}}} = -\left(\frac{\Gamma_0}{\Lambda}\frac{u_T}{w_2 - w_1}\right)^2 \frac{4\,\mathrm{sgn}\,(\Lambda)}{(G^{*2}-1)(G^{*}+z)}, \tag{4.18}$$

where

$$G^{*} = \tfrac{1}{3}(-z + \mathrm{sgn}\,(\Lambda)\,(z^2+3)^{\frac{1}{2}})$$

is just the value of G at which the slope is a maximum. The thickness (4.18) is plotted in figure 6 as a function of shock strength for upstream states having $\Lambda < 0$ and $w_1 = T_1 - T_0 = 0$. For comparison, an effective Taylor thickness Δ_{T},

$$\frac{\Delta_{\mathrm{T}}}{L_{\mathrm{d}}} = \frac{2}{3}\frac{\Gamma_0}{|\Lambda|}\frac{u_T}{w_2 - w_1} \tag{4.19}$$

has been plotted. We note that Λ does not ordinarily appear in the formula for the Taylor structure. Its appearance in (4.19) is due to the scaling with L_{d}. Inspection of figure 6 shows that the physical effects described above lead to an increase, rather than decrease, in the shock thickness with strength over the range

$$\frac{9}{8} \leqslant \frac{w_2}{u_T}\frac{|\Lambda|}{\Gamma_0} = \frac{c_{v0}}{\alpha_0 s_0 \Gamma_0}\frac{T_2 - T_0}{T_0} \leqslant \tfrac{3}{2}.$$

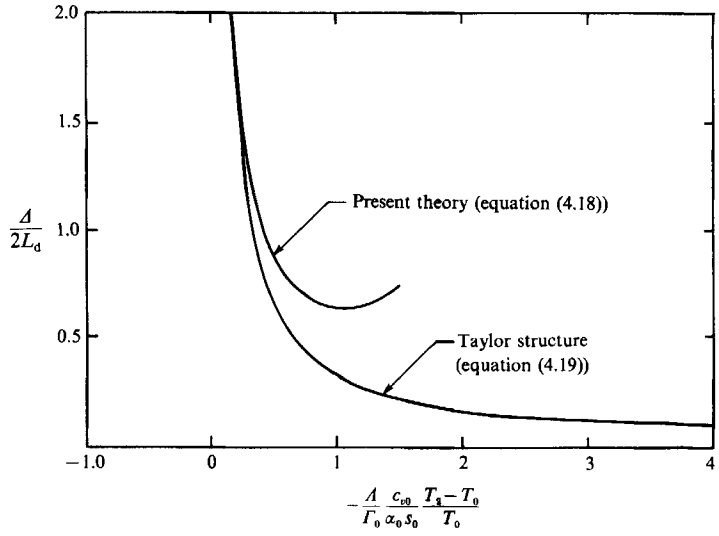

FIGURE 6. Shock thickness based on maximum-slope criterion for $\Gamma_0 > 0, \Delta < 0, w_1 = 0, T_1 = T_0$.

The right limit corresponds to the sonic shock and the left limit corresponds to the minimum in Δ as obtained by an analysis of (4.18). It is clear that the increase in thickness depicted in figures 5 and 6 could easily be mistaken for an anomolous increase in the dissipation coefficients, e.g. the bulk viscosity, or a temperature dependency of the dissipation parameters. However, because the shocks are taken to be weak, the dissipation coefficients are fixed by the undisturbed conditions T_0, p_0. The importance of the results presented here is to show that this is due to the approach to sonic conditions and should be anticipated whenever $T_0 \approx 1.88$ K.

By combining (4.12) and (4.19), it may be shown that $\Delta_T \to \infty$ as $\Gamma_0 \to 0$, i.e. the Taylor thickness diverges at the $\Gamma_0 = 0$ point. The present study shows that the higher-order terms represented by Δ must be retained when Γ is small. As a result, the actual thickness Δ remains bounded in this limit; this is easily verified by combining (4.12) with (4.18). However, because the nonlinear steepening is relatively weak, i.e. $O(\epsilon\Gamma_0) = O(\epsilon^2)$, the thickness Δ is expected to be an order $(w/u_T)^{-1}$ larger than that predicted by the Taylor theory.

5. Shock dynamics

An important difference between the present theory and that of Khalatnikov is in the more complicated existence conditions required when mixed nonlinearity is present. When (4.16) or (4.17) are satisfied, a discontinuity generated in the helium remains sharp and propagates with the shock speed σ_s. When the existence conditions are violated, there is no dissipative structure and the discontinuity suffers either a partial or total disintegration. To illustrate the former type of disintegration, we consider the case of a temperature-raising discontinuity where $\Gamma_0 > 0, \Delta < 0$ and the helium is undisturbed ahead of the discontinuity, i.e. $w_1 = 0, T_1 = T_0$. When the temperature T_ℓ immediately following the initial discontinuity satisfies

$$\frac{T_\ell - T_0}{T_0} > \frac{3}{2}\frac{\alpha_0 s_0}{c_{v0}}\frac{\Gamma_0}{|\Delta|}, \tag{5.1}$$

the sound speed behind the shock is less than the shock speed; this, of course, violates (4.17). This fact may also be verified by inspection of the plots in figure 4. If inserted in the flow this inadmissible discontinuity will split into a sonic shock and a smooth increase in temperature to T_ℓ. The temperature T_s immediately following the sonic shock is given by

$$\frac{T_s - T_0}{T_0} = \frac{3}{2}\frac{\alpha_0 s_0}{c_{v0}}\frac{\Gamma_0}{|A|}. \tag{5.2}$$

This partial disintegration is illustrated in figure 3 and is clearly evident in the experiments of Turner (1979, 1981). The significance of sonic shocks is that they are always generated by the partial disintegration of a discontinuity and, when $A < 0$, represent the shock of maximum strength.

It is a common misconception to infer that the partial disintegration of the shock necessarily occurs whenever the dynamic steepening coefficient (3.11) changes sign. If we again consider a single temperature-raising shock with $A < 0, \Gamma_0 > 0, w_1 = 0$, $T_1 = T_0$, we see that $\sigma'(T_\ell)$ becomes negative when

$$\frac{T_\ell - T_0}{T_0} > \frac{\alpha_0 s_0}{c_{v0}}\frac{\Gamma_0}{|A|},$$

where T_ℓ is again the temperature immediately following the proposed shock wave. However, the admissibility conditions (4.16*b*) permit shocks up to the sonic condition. Thus, shocks across which σ' changes sign are acceptable and will remain intact over time for

$$\frac{3}{2}\frac{\alpha_0 s_0}{c_{v0}}\frac{\Gamma_0}{|A|} \geqslant \frac{T_\ell - T_0}{T_0} > \frac{\alpha_0 s_0}{c_{v0}}\frac{\Gamma_0}{|A|}.$$

Because the shock strength is fixed for all discontinuities stronger than the sonic value, the speed of second-sound shocks in the neighbourhood of the zero of the Khalatnikov steepening parameter will be limited. As T_ℓ is continuously increased from T_0, the shock speed will increase following the parabola plotted in figure 4. Once the peak of the parabola is passed, the partial disintegration depicted in figure 3 takes place and the shock speed remains fixed for all larger values of T_ℓ. This limitation on the shock speed is compared to recent experimental results in §6.

As indicated in §3, we think this more complete understanding of the dynamics can provide the basis for relatively accurate measurements of the dependence of ρ_n on the counterflow velocity. At present, experimental data for the $\rho_n = \rho_n(w)$ relation is of the nature of an upper bound established by the accuracy of the particular experimental technique employed. However, the strength of sonic shocks is easily determined from temperature measurements similar to those presented by Turner (1981). Equations (5.2) and (3.8) may then be combined to establish the value of

$$\frac{\partial}{\partial w^2}\frac{\rho_n}{\rho} = -\frac{\partial \alpha}{\partial w^2}$$

to unprecedented accuracy.

The details of the evolution of arbitrary disturbances may be obtained by combining (3.10), (4.9) and the existence conditions (4.16) or (4.17). To conclude this section, we give a brief account of the evolution of square pulses as generated by an impulsive heat impulse; this configuration has been used in a number of experimental studies. We note that a comprehensive study of square pulses subject to (3.5) has already been given by Cramer & Kluwick (1984) and Cramer *et al.* (1986). The plots

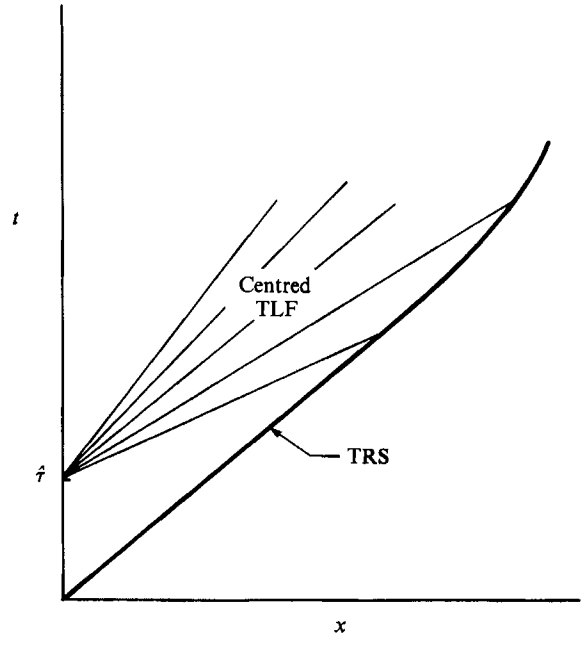

FIGURE 7. x–t diagram for case (i). TRS and TLF refer to a temperature-raising shock and a temperature-lowering fan, respectively.

found in figures 2 and 3 were generated through use of these exact solutions. The following discussion is based on an adaptation of these exact solutions to the present case.

We begin by considering a heat impulse applied at $x = 0$ and defined by

$$\begin{array}{ll} 0, & t < 0 \\ \dot{Q} > 0, & 0 < t < \hat{\tau}, \\ 0, & t > \hat{\tau}, \end{array}$$

where $\hat{\tau}$ is recognized as the period and $\dot{Q}$ = constant. We shall employ the well-known result for the slip velocity and temperature rise generated by the heater:

$$\frac{T_m - T_0}{T_0} = \frac{\alpha_0 s_0}{c_{v0}} \frac{w_m}{u_T} = \frac{\dot{Q}}{c_{v0} \rho_0 T_0 u_T}, \tag{5.3}$$

where the subscript m denotes the amplitude of the square pulse. The undisturbed helium lies in $x > 0$ and is taken to be uniform and at rest, i.e. $T = T_0, w = 0, p = p_0$, $v = 0$. We take this state to be near the high-temperature $\Gamma = 0$ locus such that $\gamma_0 > 0, A < 0$. We may then identify a total of four different evolution sequences depending on the strength of the heating. The pertinent ranges for $\dot{Q}$ are found to be

(i) $$1 \geqslant \frac{|A|}{\Gamma_0 \alpha_0 s_0 \rho_0 T_0 u_T} \dot{Q},$$

(ii) $$\tfrac{3}{2} \geqslant \frac{|A|}{\Gamma_0 \alpha_0 s_0 \rho_0 T_0 u_T} \dot{Q} \geqslant 1,$$

(iii) $$3 \geqslant \frac{|A|}{\Gamma_0 \alpha_0 s_0 \rho_0 T_0 u_T} \dot{Q} \geqslant \tfrac{3}{2},$$

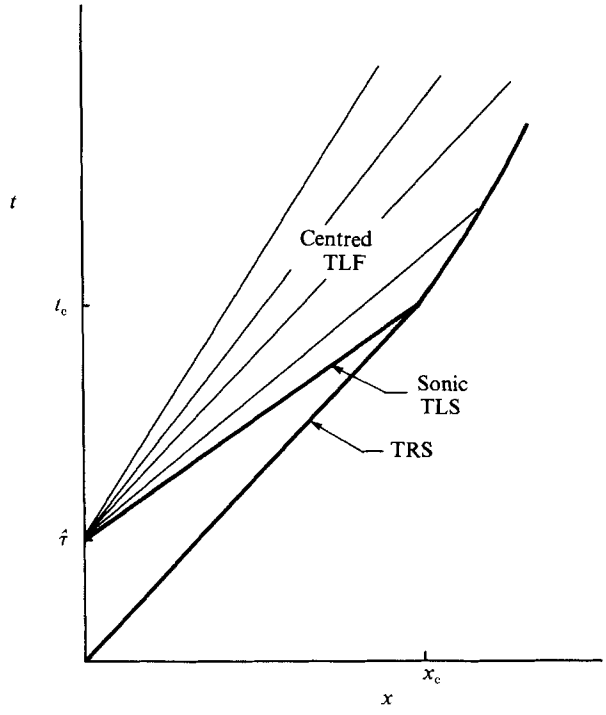

FIGURE 8. x–t diagram for case (ii). TLS denotes a temperature-lowering shock.

(iv) $$\frac{|A|}{\Gamma_0 \alpha_0 s_0 \rho_0 T_0 u_T} \dot{Q} \geqslant 3.$$

The x–t diagram for each case is sketched in figures 7–10.

In case (i) the temperature rise is relatively small and the steepening coefficient (3.11) remains positive. As a result, the general evolution is qualitatively the same as the Khalatnikov theory. When the heater is turned on, a temperature-raising shock (denoted by TRS in figures 7–10) is generated, which propagates with constant strength and speed until it is caught by the centred temperature-lowering fan (denoted by TLF) generated at $t = \hat{\tau}$. The decay law arising from the shock–fan interaction is of the general form

$$x\left(\frac{w_s}{u_T}\right)^2\left(\frac{w_s}{u_T} - \frac{3}{2}\frac{\Gamma_0}{|A|}\right) = \text{constant}, \tag{5.4}$$

where w_s is the slip velocity immediately following the shock. It is easily verified that the $x^{-\frac{1}{2}}$ decay law of the classical theory is recovered in the small-w_s limit.

In the second case, the steepening coefficient (3.11) changes sign in going from T_0 to T_m. However, the front shock satisfies the admissibility conditions (4.16b) or (4.17) and therefore remains intact as a single discontinuity. The new feature here is due to the fact that the nonlinear sound speed in the centred TLF has a local maximum where $\sigma' = 0$; this local maximum is also depicted in figure 4. As a result, the TLF folds over on itself resulting in triple-valued solutions for T and w. In the usual way, the triple-valued solutions are eliminated by inserting a temperature-lowering shock (TLS). To preserve the self-similar nature of the flow, this must be a sonic shock. Thus, in the initial stages of the evolution, the disturbance is headed by a

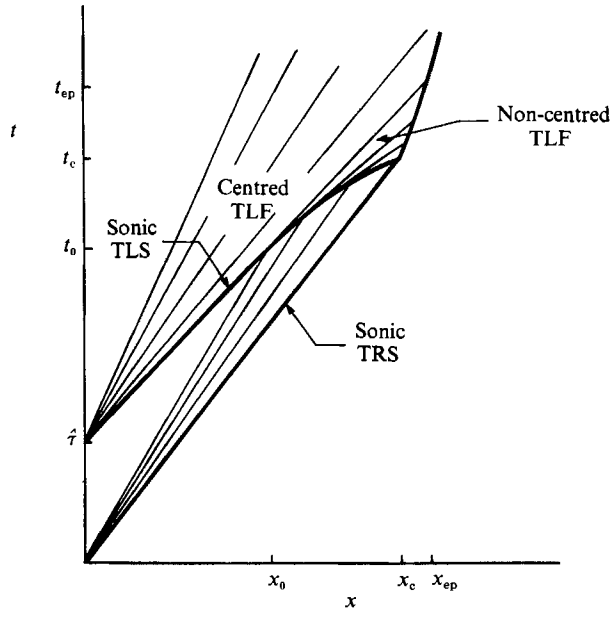

FIGURE 9. x–t diagram for case (iii).

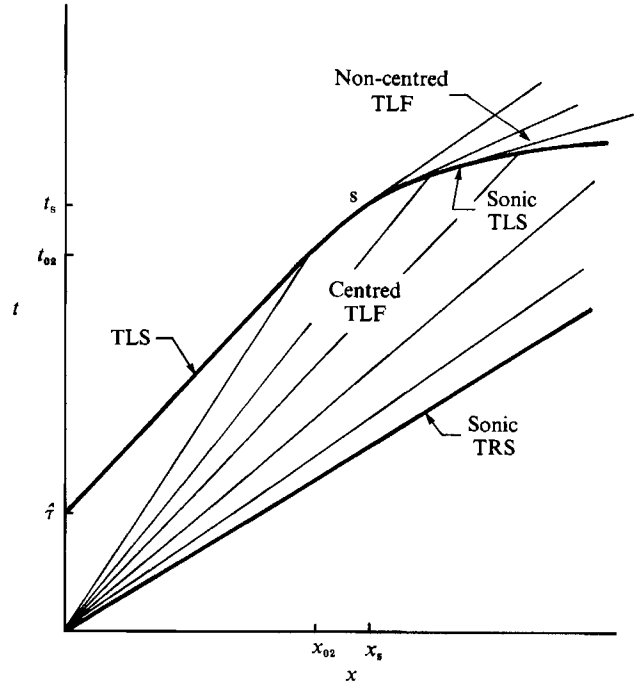

FIGURE 10. x–t diagram for case (iv). At the point marked s the rear shock becomes inadmissible and breaks up into a sonic shock and a non-centred temperature-lowering wave.

temperature-raising shock from T_0 to T_m followed by a region of uniform flow. This isothermal region is terminated by a sonic temperature-lowering shock which takes the temperature from T_m to

$$T_0\left\{1+\frac{3}{2}\frac{\Gamma_0\alpha_0 s_0}{|\Lambda|c_{v0}}\left(1-\frac{1}{3}\frac{|\Lambda|\dot{Q}}{\Gamma_0\alpha_0 s_0\rho_0 T_0 u_T}\right)\right\},$$

where the equality in (4.16a) has been combined with (5.3). The flow is then cooled to T_0 through the remainder of the centred temperature-lowering fan. Examples of the spatial distribution of T during this time period are plotted in figure 2. Experimental evidence for such a double-shock configuration is seen in the $T_0 =$ 1.865 K trace recorded by Turner (1981). The front and rear shocks eventually collide at a distance

$$x_c = \frac{24\hat{\tau}u_T|\Lambda|}{\Gamma_0^2}\left\{\frac{\dot{Q}|\Lambda|}{\Gamma_0\alpha_0 s_0\rho_0 T_0 u_T}-3\right\}^{-2}, \tag{5.5}$$

resulting in a single non-sonic temperature-raising shock. The configurations just after collision are the last two distributions seen in figure 2. As shown by Cramer & Kluwick (1984), the merged shock has a speed which is always less than either the leading or trailing shocks. Thus, speed measurements of the lead shock will show a discontinuous jump between measurement stations on either side of the collision distance x_c. After the collision, the shock decays owing to the interaction with the centred fan according to the decay law (5.4).

At heat inputs corresponding to case (iii), the admissibility conditions are no longer satisfied by the front shock. This shock then suffers a partial disintegration into a sonic temperature-raising shock and a centred temperature-raising fan. The early stages of this disintegration are seen in the first profile of figure 3 and in the $T = 1.878$ K temperature trace of Turner (1981). As depicted in figure 9 the temperature-lowering shock originating at the switch-off of the heat pulse must propagate through this fan before colliding with the front shock. The interaction with the temperature-raising fan weakens the rear shock according to the decay law

$$\frac{w_2-w_1}{u_T} = \frac{3}{2}\frac{\Gamma_0}{|\Lambda|}\left(\frac{\dot{Q}|\Lambda|}{\Gamma_0\alpha_0 s_0\rho_0 T_0 u_T}-1\right)\left(\frac{x_0}{x}\right)^{\frac{3}{8}},$$

where

$$x_0 = \frac{8\hat{\tau}u_T|\Lambda|}{3\Gamma_0^2}\left(\frac{\dot{Q}|\Lambda|}{\Gamma_0\alpha_0 s_0\rho_0 T_0 u_T}-1\right)^{-2}$$

is the value of x at which the sonic temperature-lowering shock first enters the temperature-raising fan. Because the sonic shock speeds up during the interaction, the waves in the temperature-lowering fan cannot reach the rear of the shock. Thus, for $x_c > x > x_0$, the flow immediately following the shock is due to a non-centred temperature-lowering wave. The characteristic lines in this region originate at the rear of the temperature-lowering shock and, because this shock is sonic, are constructed tangent to it. Cramer & Kluwick (1984) have referred to this as a precursor wave because it always preceeded the emitting shock in the scaled coordinates used there. These two sonic shocks eventually collide at a distance

$$x_c = \frac{32}{3}\frac{u_T\hat{\tau}|\Lambda|}{\Gamma_0^2}\left\{2\left(\frac{\dot{Q}|\Lambda|}{\Gamma_0\alpha_0 s_0\rho_0 T_0 u_T}-1\right)\right\}^{\frac{2}{3}}, \tag{5.6}$$

again resulting in a single non-sonic temperature-raising shock. After the collision, the decay of the shock is at first due to the interaction with the non-centred TLF emitted by the rear sonic shock during the time interval $t_0 \leqslant t \leqslant t_c$. This interaction is depicted in figure 9 and the resultant decay law is found to be

$$x\left(\frac{w_s}{u_T}-\frac{\Gamma_0}{|A|}\right)^{\frac{8}{3}}\left(\frac{w_s}{u_T}\right)^2 = 9\left(\frac{\Gamma_0}{4A}\right)^{\frac{8}{3}} x_c, \tag{5.7}$$

where w_s again denotes the value of w just after the shock. At $t = t_{ep}$ the interaction is complete and the remainder of the decay is through the centred fan originating at $x = 0, t = \hat{\tau}$. As in cases (i) and (ii) this final stage of the decay is governed by (5.4).

The distinguishing feature of case (iv) is that the penetration into the $\Gamma_0 < 0$ region, or, more appropriately, the $\sigma' < 0$ region, is so deep that the temperature decrease at the rear of the square pulse can be accomplished by a pure temperature-lowering shock. As indicated in figure 10, the early stages of the development are characterized by a sonic temperature-raising shock of strength and speed identical to that of case (iii) followed by a centred temperature-raising fan and then a constant-temperature region. This isothermal region is terminated by a non-sonic temperature-lowering shock. However, the interaction with the centred fan associated with the lead shock will eventually weaken the rear shock until it violates the admissibility condition (4.16*a*) or (4.17) at $x = x_s$. The rear shock then undergoes a partial disintegration into a sonic shock followed by a non-centred temperature-lowering fan. An interesting feature of this case is that the decay of the post-collision merged shock is entirely through the non-centred fan emitted by the rear shock from t_s to t_c. The collision distance for case (iv) is

$$x_c = u_T \hat{\tau}\left(\frac{2}{9}\right)^{\frac{10}{3}} \frac{|A|}{\Gamma_0^2} \frac{|A|\dot{Q}}{\Gamma_0 \alpha_0 s_0 \rho_0 T_0 u_T} \tag{5.8}$$

and the decay law for $x > x_c$ is

$$x\left(\frac{w_s}{u_T}\right)^2\left(\frac{w_s}{u_T}-\frac{\Gamma_0}{|A|}\right)^{\frac{8}{3}} = u_T \hat{\tau} 2\left(\frac{\Gamma_0}{|A|}\right)^{\frac{8}{3}} \frac{|A|}{\Gamma_0^2} \frac{|A|\dot{Q}}{\Gamma_0 \alpha_0 s_0 \rho_0 T_0 u_T},$$

which is recognized as of the same general form as (5.7).

In each of cases (ii)–(iv) the strength and speed of the leading shock remains constant until the collision with the temperature-lowering shock originating at $x = 0, t = \hat{\tau}$; this collision results in a discontinuous change in the speed and strength of the leading shock. Because the collision distance can play an important role in the interpretation of experimental results we have plotted the x_c *vs.* $\dot{Q}$ relations given in (5.5), (5.6) and (5.8) in figure 11. The dashed line in this figure is not a collision distance but the distance at which the centred fan first catches the lead shock in case (i). Its significance is similar to the collision distances in that it marks the distance at which the front shock first begins to weaken and slow. This interaction distance is given by

$$x = \frac{2\hat{\tau} u_T |A|}{\Gamma_0^2}\left(\frac{|A|\dot{Q}}{\Gamma_0 \alpha_0 s_0 \rho_0 T_0 u_T}\right)^{-1}\left(1-\frac{2}{3}\frac{|A|\dot{Q}}{\Gamma_0 \alpha_0 s_0 \rho_0 T_0 u_T}\right)^{-1}. \tag{5.9}$$

We note that the minimum interaction distance occurs when

$$\dot{Q} = \frac{3}{4}\frac{\Gamma_0 \alpha_0 s_0 \rho_0 T_0 u_T}{|A|},$$

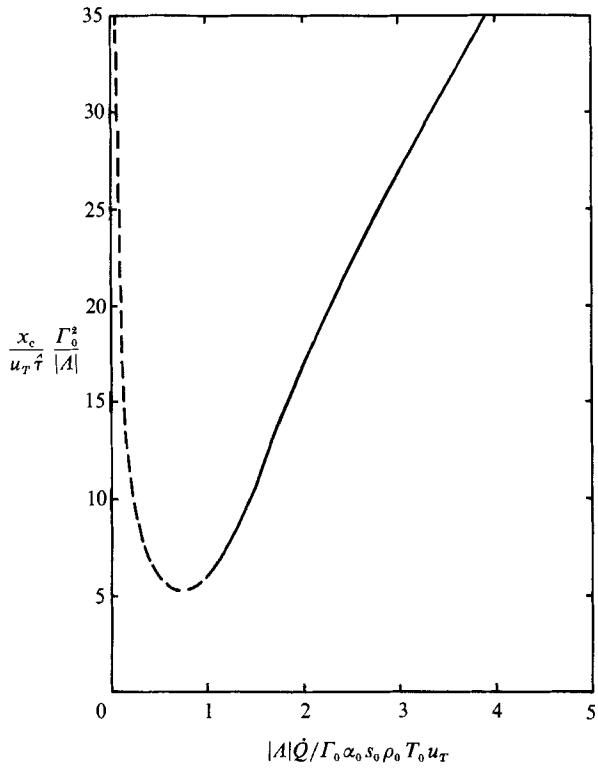

FIGURE 11. Variation of collision distance with $\dot{Q}$. The solid line represents equations (5.5), (5.6) and (5.8). The dashed line represents the distance at which the shock first begins interacting with the centred fan in case (i).

which yields a minimum distance of

$$x_{\min} = \tfrac{16}{3} u_T \hat{\tau} \frac{|A|}{\Gamma_0^2}. \tag{5.10}$$

As an example, we consider the small-Γ case ($T_0 = 1.86$ K) studied by Cummings, Schmidt & Wagner (1978). As in §6, we take $u_T = 19.29$ m/s, $\Gamma_0 \approx 0.0775$ and A to be the value at 1.884 K. (To the accuracy inherent in (3.5) and (3.8) we may evaluate A either at the actual undisturbed state or at the zero of Γ.) We then find that (5.10) may be approximated by

$$x_{\min} = 15.97\hat{\tau},$$

where x is in mm and $\hat{\tau}$ is in μs. For the 50 μs pulse used to generate figure 8 of their study we find that $x_{\min} \approx 798$ mm which is over ten times larger than any of the distances employed. Thus, we would not expect to see any decrease (whether continuous or discontinuous) in the shock speed with $\dot{Q}$ in the 1.86 K series of experiments; this appears to be consistent with the data presented by Cummings and co-workers.

It is of interest to contrast (5.9) with the corresponding result of the Khalatnikov theory:

$$x = \frac{2\hat{\tau} u_T}{\Gamma_0} \frac{\alpha_0 s_0 \rho_0 T_0 u_T}{\dot{Q}},$$

which predicts that the interaction distance decreases monotonically with the magnitude of the heat input. The local minimum illustrated in figure 11 corresponds to a maximum speed difference between the temperature-raising shock and the leading edge of the temperature-lowering fan. The fact that such a maximum is inevitable in the present theory can also be seen by inspection of the nonlinear sound and shock speeds plotted in figure 4. The collision distances are also seen to increase monotonically with $\dot{Q}$. This can again be explained by a detailed examination of the relative shock speeds. In fact, the speed of the leading shock is fixed after becoming sonic at

$$\dot{Q} = \frac{3}{2}\frac{\Gamma_0 \alpha_0 s_0 \rho_0 T_0 u_T}{|A|},$$

while the initial speed of the trailing shock continues to decrease. For heat fluxes greater than

$$2\frac{\Gamma_0 \alpha_0 s_0 \rho_0 T_0 u_T}{|A|},$$

the initial speed of the trailing shock is actually less than that of the leading shock. At these levels, the two shocks are actually moving away from each other rather than towards each other. The trailing shock only begins to catch the lead shock after being accelerated by the interaction with the temperature-raising fan.

As a second example of our results, we examine the conditions required for the experimental detection or observation of the collision process. We consider an undisturbed temperature of 1.825 K. We again evaluate Γ_0 using a graphical interpolation, A at 1.884 K and all other parameters by averaging the values at 1.80 and 1.85 K. As a result,

$$\frac{\Gamma_0^2}{u_T|A|} = 1.768\frac{\mu s}{mm} \quad \text{and} \quad \frac{\Gamma_0 \alpha_0 s_0 \rho_0 T_0 u_T}{|A|} = 38.69\frac{W}{(cm)^2}.$$

If we consider a pulse of duration $\hat{\tau} = 20$ μs and $\dot{Q} = 36$ W/cm^2 and employ (5.9) we find that the interaction between the leading shock and the temperature-lowering fan begins at 64.0 mm. A collision of the type described in case (ii) occurs for a pulse of the same duration and $\dot{Q} = 46$ W/cm^2 at a distance from the heater of 82.8 mm. The collision between two sonic shocks described in case (iii) occurs for $\hat{\tau} = 20$ μs, $\dot{Q} =$ 69 W/cm^2 at 162.8 mm. It therefore appears that the observation of the evolution of double shocks up to and including collisions is entirely possible within the constraints of current technology.

6. Comparison with experimental studies

In this section, we compare the results of the present theory to recent experimental studies. The first set are those of T. N. Turner. Although no shock strengths were given corresponding to the temperature profiles presented in the 1981 article, the qualitative features are all in agreement with the present theory, including the general ordering of the profiles, the order of magnitudes involved and the direction of the curvature of the temperature variation. Our results also appear to be qualitatively consistent with the experiments of Torczynski *et al.* (1984).

More extensive comparisons can be made with the signal-speed measurements of Cummings *et al.* (1978). The present theory is expected to be in reasonable agreement with the data at 1.86 K. The undisturbed state is fairly close to the $\Gamma_0 = 0$ point and

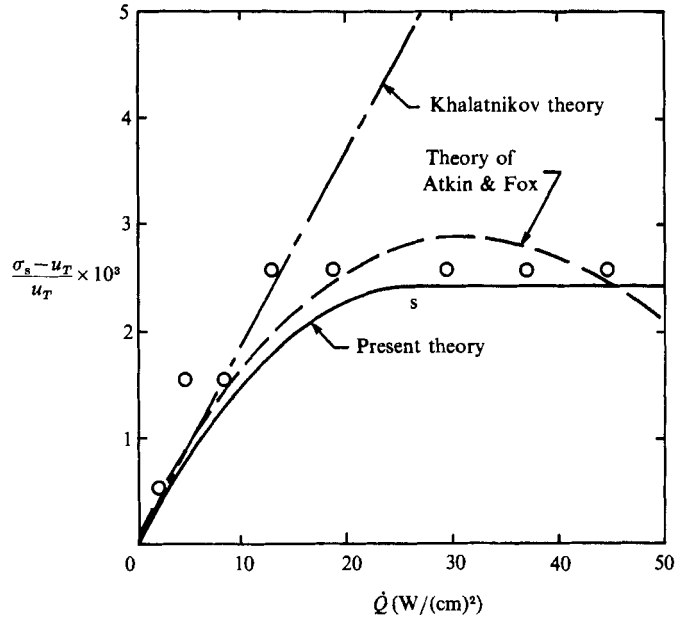

FIGURE 12. Variation of signal speed with heat input at $T_0 = 1.86$ K. The circles denote data points from Cummings *et al.* (1978). For heat inputs beyond the point marked s the strength of the lead shock is fixed at the sonic value.

the experiments of Turner (1981) show that mixed nonlinearity, relatively free of the effects of quantum turbulence, may be attained in the neighbourhood of this bath temperature. The experimental data of Cummings *et al.*, along with the results of the present theory, are plotted in figure 12. The formulae used to plot the present theory are

$$\frac{\sigma_s - u_T}{u_T} = \frac{\Gamma_0^2}{|A|} \begin{cases} \frac{1}{2}q(1-\frac{1}{3}q) & \text{for } 0 \leqslant q \leqslant \frac{3}{2}, \\ \frac{3}{8} & \frac{3}{2} \leqslant q, \end{cases} \tag{6.1}$$

where

$$q \equiv \frac{|A|\,\dot{Q}}{\Gamma_0 \alpha_0 s_0 \rho_0 T_0 u_T} \tag{6.2}$$

is a non-dimensional heat flux. At the lower heat fluxes the shock is non-sonic and follows the parabola plotted in figure 4. At $q = \frac{3}{2}$ the shock becomes sonic. As discussed in §5, the shock strength and speed then become fixed at the sonic value. Our calculations indicate that this occurs at a $\dot{Q} \approx 26.1$ W/cm² when the undisturbed state is 1.86 K. The numerical values for $\alpha_0 s_0 \rho_0 T_0 u_T$, Γ_0 and A were found to be 209.25 W/cm², 7.75×10^{-2} and -0.9322, respectively. The first was obtained by a straightforward linear interpolation between 1.85 K and 1.9 K. As pointed out in the previous section, the value of A may be taken to be that at 1.884 K with no loss in generality. It was found that linear interpolation of Γ_0 was not sufficiently accurate when Γ_0 is small, so a more accurate graphical interpolation was used instead. The experimental points were taken from the original tabular data rather than the plots of Cummings *et al.* (1978). This tabular data was kindly transmitted to the authors by R. J. Atkin and is displayed in table 2. It should be noted that the original data were only recorded to four significant digits. The equality of the signal speeds at 4.70 and 8.35 W/cm² is therefore likely to be due to the round-off process. To further place our results in the context of these experiments we have compared our speeds, rounded off to the same accuracy, to those of Cummings *et al.* in table 2.

$\dot{Q}$ (W/cm²)	$\sigma_s\|_{exp}$ (m/s)	$\sigma_s\|_{cal}$ (m/s)
0	19.29	—
2.09	19.30	19.30
4.70	19.32	19.30
8.35	19.32	19.32
13.05	19.34	19.32
18.80	19.34	19.32
29.36	19.34	19.34
37.71	19.34	19.34
44.66	19.34	19.34

TABLE 2. Tabular data of Cummings *et al.* (1978) for the signal speed. Calculated values ($\sigma_s|_{cal}$) are obtained from equations (6.1), (6.2) with the indicated numerical values. The complete results were then rounded off to the accuracy of the experimental data.

For purposes of comparison we have also plotted the results of the Khalatnikov theory

$$\frac{\sigma_s - u_T}{u_T} = \frac{1}{2}\frac{\Gamma_0 \dot{Q}}{\alpha_0 s_0 \rho_0 T_0 u_T}$$

and, with a dashed line, the theoretical results of Atkin & Fox (1984). The formulae used in plotting Atkin & Fox's theory are the parametric equations

$$\frac{\sigma_s - u_T}{u_T} = \frac{3.8\Delta T - 65(\Delta T)^2}{19.29}$$
$$\dot{Q} = 955\Delta T + 4025(\Delta T)^2, \tag{6.3}$$

where ΔT is the induced temperature rise in K and $\dot{Q}$ is in W/cm². The numerical coefficients are those used by Atkin & Fox (1984) in their figure 2. There are two primary differences between our theory and that of Atkin & Fox. The first is that Atkin & Fox have taken ρ = constant and v = constant, whereas we make no restrictions on the variation of the bulk density and speed. As a result, Atkin & Fox do not account for the first-order (the linear theory is the zeroth-order) pressure and density perturbations generated by nonlinear effects. Although these perturbations can be ignored in the Khalatnikov theory, a careful examination of the derivation of (3.8) shows that they are essential for the computation of the second nonlinearity coefficient A. However, the numerical error involved in neglecting the induced density perturbations appears to be moderate. For example, the difference between our A and an effective coefficient based on Atkin & Fox's u_2 is only about 12.5% at 1.884 K. We should note that the Khalatnikov parameters of each theory are identical, although there appears to be small differences in the numerical estimation. The second difference between our theory and that of Atkin & Fox is that they did not consider the flow surrounding the shock, nor did they examine the dissipative structure. Thus, their work does not take into account the fundamental existence conditions and therefore the partial disintegration and speed-limiting processes found in the experimental studies quoted here.

On the basis of these comparisons we conclude that the theory presented here provides a reasonable quantitative as well as qualitative model for second-sound propagation in the neighbourhood of the zero of the Khalatnikov steepening parameter. It also appears reasonable to conclude that the speed limitation seen in

the 1.86 K series runs of Cummings *et al.* (1978) is the partial disintegration of the lead shock described in previous sections. This mechanism was first identified by Turner (1983) who referred to this as the wave dynamic limit.

We do not expect any agreement between our results and the experiments at the higher bath temperatures. For example, at $T_0 = 1.759$ K, we estimate $\Gamma_0 \approx 0.35$, which is likely to be too large for the present theory. More importantly, the slip velocities based on (5.3) exceed the critical velocities identified by Turner (1983) at values of $\dot{Q}$ exceeding 26 W/cm^2; see, for example, figure 17 of Turner (1983). Because the breakdown of the superfluidity has taken place long before the mechanisms described here can take effect, the agreement between experiment and theory is poor. In particular, our theory yields values of the maximum speed difference that are 2.5 times larger than the observed values.

7. Summary

It has been shown that the nonlinear propagation of second sound is governed by the cubic Burgers' equation (4.3) when the undisturbed state is in the neighbourhood of one of the zeros of the quadratic nonlinearity parameter (1.3). Numerical values for the new nonlinearity parameter A were estimated through use of the tabular data of Maynard (1976) and Khalatnikov's (1952) theoretical estimate of the $\rho_n = \rho_n(w)$ relation. Solutions to (3.5) or (4.3) combined with the numerical estimates of (3.8) are in reasonable quantitative and qualitative agreement with the experimental results of Turner (1979, 1981), Torczynski *et al.* (1984) and Cummings *et al.* (1978).

An important observation is that the second nonlinearity parameter must be taken to be the dynamic parameter A rather than the static parameter based on the slope of the Γ *vs.* T curve. As a result, mixed nonlinearity (in the sense of simultaneous forward and backward steepening) is possible in disturbances having strictly positive (or strictly negative) values of the Khalatnikov steepening coefficient Γ at every point in the disturbance. The reason for the difference between (3.8) and (3.13) is that (1.3) is only an approximation to the exact steepening coefficient. A careful inspection of the derivation of (3.7) shows that terms neglected in (1.3) make a non-zero contribution to (3.8). In retrospect, it would be surprising if simple differentiation of (1.3), which is the steepening coefficient evaluated at the undisturbed state $p = p_0, T = T_0, w = 0$, would yield the correct parameter.

The present study leaves the results of the Khalatnikov ($\Gamma_0 = O(1)$) theory unchanged. Even when $\Gamma_0 = o(1)$, the direction of steepening of sufficiently weak waves will still be determined by the sign of Γ_0. In waves of larger amplitude, the more complete model based on (3.5) or (4.3) will be required for purposes of predicting and describing mixed nonlinearity.

Results of further interest in the non-dissipative theory are the expressions for the shock speed (4.9) and the existence conditions for weak second-sound shocks involving mixed nonlinearity. The conditions (4.16) or (4.17) are expected to be both sufficient and necessary for the existence of shocks near the $\Gamma_0 = 0$ locus. This is because these were based on the existence of a dissipative structure which automatically takes into account the irreversible portion of the entropy increase across the shock.

The authors have profited by a number of stimulating conversations with Drs T. N. Turner and R. J. Atkin. Their comments and suggestions have led to significant improvements to this work and are greatly appreciated.

Appendix. General evolution equation

We consider a general quasi-linear, strictly hyperbolic system of the form

$$u_{i\bar{t}} + A_{ij}(u_p)\, u_{j\bar{x}} = 0. \tag{A 1}$$

As in the body of this report, we employ the Einstein summation convention and the subscripts $\bar{x}, \bar{t}$ refer to partial derivatives with respect to space and time. The solution vector is $N \times 1$ and the speed matrix A_{ij} is $N \times N$. The italic indicies will range from 1 to N. As in Taniuti & Wei (1968), we assume small disturbances to a uniform rest state so that

$$u_i = u_i^0 + \epsilon u_i^1 + O(\epsilon^2),$$

where u_i^0 is a constant vector and $u_i^1(\bar{x}, \bar{t})$ is the disturbance. The non-dimensional small parameter ϵ is a measure of the disturbance amplitude. The evolution equation derived by Taniuti & Wei (1968) is just the inviscid Burgers' equation

$$U_t + \epsilon \Gamma U U_X = 0, \tag{A 2}$$

where Γ is an order-one constant characterizing the system (A 1) and the undisturbed state. The spatial variable X is $\bar{x} - \lambda \bar{t}$, where λ is an eigenvalue of $A_{ij}(u_i^0)$. In the present study Γ is chosen to be $O(\epsilon)$. To lowest order (A 2) implies that no steepening is noticeable over the times considered by Taniuti & Wei, i.e. ϵ^{-1}. The actual steepening will be seen at times of order $(\epsilon\Gamma)^{-1} = O(\epsilon^{-2})$. Furthermore, certain terms neglected, and therefore not shown, in (A 2) will make contributions equal to that of the quadratic term shown.

Teymur & Suhubi (1978) have presented a method of accounting for the higher-order terms when the speed matrix A_{ij} is of special form. However, the required conditions are not satisfied in general problems and, in particular, the superfluid system.

Sen & Cramer (1987) have shown that the general extension of (A 2) when $\Gamma = O(\epsilon)$ is

$$U_\tau + (\hat{\Gamma} + \tfrac{1}{2}\Lambda U)\, U U_X = 0, \tag{A 3}$$

where the subscripts denote differentiation with respect to $\tau = \epsilon^2 \bar{t}$ and $X = \bar{x} - \lambda \bar{t}$ and

$$\hat{\Gamma} = \frac{l_i B_{ijk} r_j r_k}{\epsilon l_m r_m}, \tag{A 4}$$

$$\Lambda = \frac{2 l_i C_{ijkl} r_j r_k r_l - (2 d_\sigma + e_\sigma) B^{\mathrm{c}}_{\sigma jk} r_j r_k}{l_m r_m}. \tag{A 5}$$

The constant vectors l_i and r_i are the left and right eigenvectors to the linearized A_{ij} matrix; i.e.

$$(A^0_{ij} - \lambda \delta_{ij})\, r_j = 0, \quad (A^0_{ij} - \lambda \delta_{ij})\, l_i = 0, \tag{A 6}$$

where δ_{ij} is the Kronecker delta and $A^0_{ij} \equiv A_{ij}(u^0_p)$. As in the work of Taniuti & Wei, the eigenvalue λ is just the non-dimensional version of the linear wavespeed. The quantities $B_{ijk}, B^{\mathrm{c}}_{ijk}, C_{ijkl}$ are defined

$$\begin{aligned} B_{ijk} &\equiv \frac{\partial A_{ij}}{\partial u_k}(u^0_p), \quad B^{\mathrm{c}}_{ijk} \equiv \frac{\partial A_{ij}}{\partial u_k}(u^{\mathrm{c}}_p) \\ C_{ijkl} &\equiv \frac{1}{2}\frac{\partial A_{ij}}{\partial u_k \partial u_l}(u^{\mathrm{c}}_p) \approx \frac{1}{2}\frac{\partial A_{ij}}{\partial u_k \partial u_l}(u^0_p). \end{aligned} \tag{A 7}$$

The vector u_p^c is the state at which $\Gamma \equiv 0$, i.e.

$$l_i r_j r_k B_{ijk}^c \equiv 0. \tag{A 8}$$

The quantities d_α, e_α, each of which is $(N-1)\times 1$, are determined by solving the following linear systems

$$R_{\alpha\beta} d_\beta = S_{\alpha m} b_m, \quad R_{\alpha\beta} e_\beta = S_{\alpha m} c_m \tag{A 9}$$

where $R_{\alpha\beta} \equiv S_{\alpha j} S_{\beta j}$ and $S_{\alpha i}$ is an $(N-1)\times N$ array formed by the $(N-1)$ linearly independent rows of the singular matrix $A_{ij}^0 - \lambda \delta_{ij}$. In (A 5) and (A 9) the Greek indicies take on these $(N-1)$ values. The remaining quantities found on the right-hand sides of (A 9) are defined by

$$b_i \equiv B_{piq}^c l_p r_q, \quad c_i \equiv B_{pqi}^c l_p r_q. \tag{A 10}$$

To the accuracy required here, B_{ijk}^c may be replaced by B_{ijk}^0 in (A 10). Finally, we note that the lowest-order solution to (A 1) is

$$u_i = u_i^0 + \epsilon r_i U + O(\epsilon^2).$$

All of the quantities appearing in (A 3) are of order one. To verify this for $\hat{\Gamma}$, we note that

$$B_{ijk} \equiv \frac{\partial A_{ij}}{\partial u_k}(u_p^0) = \frac{\partial A_{ij}}{\partial u_k}(u_p^c) + O(\epsilon) = B_{ijk}^c + O(\epsilon).$$

Hence,

$$l_i (B_{ijk} - B_{ijk}^c) r_j r_k = O(\epsilon).$$

The result that $l_i B_{ijk} r_j r_k = O(\epsilon)$ then follows immediately from (A 8).

A comparison of (A 4) with the results of Taniuti & Wei (1968) reveals that $\hat{\Gamma}$ will always be the value of Γ appearing in (A 2) divided by ϵ. This is verified in the present study and in the independent calculations of Cramer & Kluwick (1984).

The effects of weak dissipation and weak dispersion were also discussed by Sen & Cramer (1987). It is shown that the appropriate dissipation and dispersion coefficients are simply carried over from either the linear or $\Gamma = O(1)$ theory. The case of dissipation is illustrated in the present study.

The new feature here is the general algorithm for the calculation of the cubic nonlinearity coefficient A. The portion of this involving C_{ijkl} is clearly due to the higher-order terms in the expansion of the speed matrix A_{ij}. The terms involving d_σ and e_σ arise because the higher-order terms in the perturbation expansion of u_i necessarily make a contribution to the final value of A. Thus, in addition to solving the linearized problem for $u_i^1 (= r_i U)$, it was necessary to determine the particular solution for the first correction u_i^2. The reduced linear equations (A 9) are a direct result of the singular nature of the inhomogeneous problem for u_i^2. For further details, the reader is referred to the original study by Sen & Cramer (1987).

REFERENCES

Atkin, R. J. & Fox, N. 1984 The dependence of thermal shock wave velocity on heat flux in helium II. *J. Phys.* C: *Solid State Phys.* **17**, 1191–1198.

Cramer, M. S. 1987 Structure of weak shocks in fluids having embedded regions of negative nonlinearity. *Phys. Fluids* **30**, 3034–3044.

Cramer, M. S. & Kluwick, A. 1984 On the propagation of waves exhibiting both positive and negative nonlinearity. *J. Fluid Mech.* **142**, 9–37.

Cramer, M. S., Kluwick, A., Watson, L. T. & Pelz, W. 1986 Dissipative waves in fluids having both positive and negative nonlinearity. *J. Fluid Mech.* **169**, 323–336.

CRIGHTON, D. G. 1986 The Taylor internal structure of weak shock waves. *J. Fluid Mech.* **173**, 625–642.

CUMMINGS, J. C., SCHMIDT, D. W. & WAGNER, W. J. 1978 Experiments on second-shock waves in superfluid helium. *Phys. Fluids* **21**, 713–717.

DESSLER, A. J. & FAIRBANK, W. M. 1956 Amplitude dependence of the velocity of second sound. *Phys. Rev.* **104**, 6–10.

DONNELLY, R. J. & SWANSON, C. E. 1986 Quantum turbulence. *J. Fluid Mech.* **173**, 387–429.

FISZDON, W. & VOGEL, H. 1986 Selected problems of hydrodynamics of liquid helium. *Z. Angew. Math. Mech.* **66**, T9–T18.

GARRETT, S. 1981 Nonlinear distortion of the 4th sound in superfluid ^{3}He-B. *J. Acoust. Soc. Am.* **69**, 139–144.

KHALATNIKOV, I. M. 1952 Discontinuities and large amplitude sound waves in helium II. *Zh. Eksp. Teor. Fiz.* **23**, 253.

KHALATNIKOV, I. M. 1965 *An Introduction to the Theory of Superfluidity.* W. A. Benjamin.

KOJIMA, H., VEITH, W., GUYON, E. & RUDNICK, I. 1976 Superfluid density in the presence of persistent current in superfluid ^{4}He. *J. Low Temp. Phys.* **25**, 195–217.

LANDAU, L. D. & LIFTSHITZ, E. M. 1959 *Fluid Mechanics.* Pergamon.

LEE-BAPTY, I. P. 1981 Nonlinear wave propagation in stratified and viscoelastic media. Ph.D. dissertation, Leeds University, UK.

LEE-BAPTY, I. P. & CRIGHTON, D. G. 1987 Nonlinear wave motion governed by the modified Burgers equation. *Phil. Trans. R. Soc. Lond.* A **323**, 173–209.

LIEPMANN, H. W. & LAGUNA, G. A. 1984 Nonlinear interactions in the fluid mechanics of helium II. *Ann. Rev. Fluid Mech.* **16**, 139–177.

LIEPMANN, H. W. & TORCZYNSKI, J. R. 1985 Shock waves in helium at low temperatures. In *Proc. 15th Intl Symp. on Shock Tubes and Waves* (ed. D. Bershader & R. Hanson), pp. 87–96. Stanford University Press.

MAYNARD, J. 1976 Determination of the thermodynamics of helium II from sound-velocity data. *Phys. Rev.* B **14**, 3868–3891.

PUTTERMAN, S. J. 1974 *Superfluid Hydrodynamics.* North-Holland.

ROBERTS, P. H. & DONNELLY, R. J. 1974 Superfluid mechanics. *Ann. Rev. Fluid Mech.* **6**, 179–225.

SEN, R. & CRAMER, M. S. 1987 A general scheme for the derivation of evolution equations describing mixed nonlinearity. *VPI&SU Engineering Rep.* no. VPI-E-87-16.

TANIUTI, T. & WEI, C.-C. 1968 Reductive perturbation method in nonlinear wave propagation. *J. Phys. Soc. Japan* **24**, 941–946.

TEYMUR, M. & SUHUBI, E. 1978 Wave propagation in dissipative and dispersive non-linear media. *J. Inst. Maths. Applics.* **21**, 25–40.

THOMPSON, P. A., CAROFANO, G. C. & KIM, Y.-G. 1986 Shock waves and phase changes in a large-heat-capacity fluid emerging from a tube. *J. Fluid Mech.* **166**, 57–92.

TORCZYNSKI, J. R., GERTHSEN, D. & ROESGEN, T. 1984 Schlieren photography of second-sound shock waves in superfluid helium. *Phys. Fluids* **27**, 2418–2423.

TURNER, T. N. 1979 Second-sound shock waves and critical velocities in liquid helium II. Ph.D. dissertation, California Institute of Technology, Pasadena.

TURNER, T. N. 1981 New experimental results obtained with second-sound shock waves. *Physica* B **107**, 701–702.

TURNER, T. N. 1983 Using second-sound shock waves to probe the intrinsic critical velocity of liquid helium II. *Phys. Fluids* **26**, 3227–3241.